**ASIAN JOURNAL OF CIVIL ENGINEERING (BHRC) VOL. 16, NO. 3 (2015)**
**PAGES 383-415**

# SEISMIC POUNDING OF ADJACENT LINEAR ELASTIC BUILDINGS WITH VARIOUS CONTACT MECHANISMS FOR IMPACT SIMULATION

Nilesh U. Mate, S. V. Bakre* and O. R. Jaiswal
Applied Mechanics Department, Visvesvaraya National Institute of Technology, Nagpur 440010, India

**Received:** 4 March 2014; **Accepted:** 20 October 2014



## ABSTRACT

This paper presents the comparative study of pounding response of multi-degree-of-freedom (MDOF) system by using various impact simulation techniques. The prediction of impact response of three adjacent MDOF stick system is carried out by means of spring-dashpot contact element, which will be activated only when the masses of adjacent structures comes in contact. The stick model study is entirely being made on MATLAB programming tool. The few sets of obtained response of MATLAB programs are also been compared with the SAP results for the validation purpose. The entire investigation has been done by using nonlinear step by step time history method.
The result indicates that the nonlinear contact spring impact simulation models give lesser magnitude pounding forces than that of linear contact spring impact simulation models, but as far as their numbers are concerned, they are marginally same in both the types. It was also noticed that in the exterior right flexible structure subjected to pounding for series of structures, the applied ground excitations offers unconventional pattern of absolute shear forces. That means the top storey of the exterior rigid structure during pounding may offer more values of shear forces than the immediately lower storeys.

**Keywords:** Seismic pounding; impact simulation models; gap element; MDOF stick system; time history analysis; structural energy.

## 1. INTRODUCTION

As time passed and population of cities increased, the civil structures expands are erected horizontally and vertically to meet human demands, due to presence of these tall and massive structures in the seismically active area the structural failure conditions became

*E-mail address of the corresponding author: svbakre@apm.vnit.ac.in (S. V. Bakre)

more severe. The number of buildings in modern cities constructed rapidly to fulfill the human needs and most of the times the structures are normally constructed in close proximity to each other. This creates a new problem in structural engineering called as mutual pounding of adjacent buildings during occurrences of natural tremors like earthquakes. In practice, adjacent structures tremble out of phase due to different dynamic characteristics. Moreover, in current design process, adjacent buildings with insufficient clear spacing are designed as a standalone structure by ignoring the pounding action during earthquake loading. This negligence causes failure of structures. This is because of huge amount of additional shear forces and bending moments developed in the columns due to repeated impulsive actions during tremor.

Investigations of past and recent earthquakes damage have illustrated several instances of pounding damage in both building and bridge structures [1,2,3]. The survey conducted by Rosenblueth and Meli [1], after the earthquake that struck Mexico City in 1985 revealed that pounding was present in over 3 to 4.5% of the 330 collapsed or severely damaged buildings surveyed, and in 15% of all cases that suffered major damages. This earthquake illustrated the significant seismic hazard of pounding, with the largest number of buildings damaged by this effect during a single earthquake. Kasai et al. [2] have investigated the pounding damage in the San Francisco Bay area during the 1989 Loma Prieta earthquake also revealed widespread pounding incidents. Unlike the damage to buildings in earthquake affected regions, where a large number of injuries or deaths were caused directly by building collapse, bridge damage isolated the affected area by preventing the transport of lifeline supplies and denying access by rescuers. This generated an even a more severe problem with huge burden on society. The majority of buildings located in Indian cities are very closely-spaced without adequate seismic separation. Such a building stock has to be identified and analyzed with reference to its vulnerability to earthquake damage to facilitate actions taken for its strengthening, and retrofitting to minimize pounding in case of earthquake occurrence. Gokhale and Joshi [3], have studied the potential hazard of buildings located on old districts of historic city of Pune. Out of 450 surveyed buildings, 357 buildings were found with zero separation while rests of them have a little separation. Based on the survey data and evaluation of potential pounding damage, it is found that out of 450 surveyed buildings 14% will suffer pounding damage. Among them 2.4% will collapse, 4.1% will suffer severe damage, 3.6% will suffer medium damage, while rest of them will suffer minor damage.

In recent times, the phenomenon of pounding between buildings during earthquakes has been rigorously studied by applying various structural models and using different contact mechanism for impact simulations, [4-15]. Studies of seismic pounding typically utilize the lumped mass model [4-11], where the building floors are assumed as rigid diaphragms with lumped seismic masses. Early works for the idealization of the pounding phenomenon have utilized Single Degree-Of-Freedom (SDOF) oscillators in order to simplify the problem and produce some qualitative results on the behavior of structures under pounding [4,5,6,7,8]. The mathematical models are further being simplified by taking up two dimensional analyses as well as three dimensional analyses [11,12,13,14,15].

The fundamental study on pounding between adjacent buildings in series was conducted by Anagnostopoulos [4], wherein the structures were modeled by SDOF and collisions are simulated with the help of the linear viscoelastic model of impact force. A parametric

investigation of the problem stated by the author in published paper shows that the end structures experience almost and always substantial increases in their response while for 'interior' that could not happens. Pantelides and Ma [5] have studied the dynamic behavior of damped SDOF elastic and inelastic structural systems with one-sided pounding during an earthquake, to capture the pounding in their research work; they have used the Hertz contact gap element. The effects of separation distance and inelastic structural behavior on the magnitude of the pounding force were examined in this research paper. Most of actual poundings in the past are likely to be eccentric due to asymmetric structural plans or non-constant gaps between adjacent buildings. Seismic torsional pounding is a highly nonlinear phenomenon in nature. This type of study was conducted by Wang and Chau [6] for the impacts between two single-story asymmetric towers by adopting the nonlinear Hertz contact law for impact simulation. From the numerical simulation results it was observed that torsional pounding tends to be much more complex than translational pounding, and most of torsional impacts are chaotic. Numerical investigations were also been performed in the past on a pounding system that consists of a damped single-degree-of-freedom (SDOF) structure and a rigid barrier. This kind of study was performed by Davis [7]. In published literature, the Hertz contact model was used to simulate pounding behavior.

With the development of structural health monitoring, the on-line detection of pounding becomes possible. The detection of pounding can provide useful information of potential damage of structures. Xing et al.,[8] have used wavelet scalograms of dynamic response to detect pounding and also examined the feasibility of this method. Numerical investigations were performed on a pounding system that consisted of a damped single-degree-of-freedom (SDOF) structure and a rigid barrier. Hertz contact model was used to simulate pounding behavior. The wavelet scalograms of acceleration responses were used to identify poundings. It was found that the scalograms can indicate the occurrence of pounding and occurrence time very well.

Maison and Kasai [9], develops a Multi-Degree-Of-Freedom (MDOF) models, with each storey's mass lumped on the floor level to study the response of unequal heights of a light high-rise building, colliding against a massive low rise structure. In their research work, a single linear spring was being placed at the roof level of the lower structure. Study shows that pounding generates drifts, shears, and overturning moments in the stories above the pounding location that are greater than those from the case where pounding hasn't occurred. Kun et al.,[10] proposed a modified Kelvin impact model for pounding simulation of base isolated buildings (BIB) with adjacent structures. Relevant parameters in the modified Kelvin model were theoretically derived and numerically verified by the authors through a simple pounding case. At the same time, inelasticity of the isolated superstructure was introduced in order to accurately evaluate the potential damage to the superstructure caused by the pounding of the BIB with adjacent structures.

In the research article by Moustafa and Mahmoud [11], the pounding of adjacent buildings was assessed using input energy, dissipated energy and damage indices. Damage indices (DI) were computed by comparing the structure's responses demanded by earthquakes and the associated structural capacities. Damage indices provide quantitative estimates of structural damage level, and thus, a decision on necessary repair can be taken. Adjacent buildings with fixed-base and isolated-base were considered by the authors. The nonlinear viscoelastic model was used for capturing the induced pounding forces.

Papadrakakis and Mouzakis [12] have investigated the linear and nonlinear structural response for the 3-D pounding phenomenon of two adjacent buildings during earthquakes with aligned rigid horizontal diaphragms. The developed formulation takes into account three dimensional dynamic contact conditions for the velocities and accelerations based on the impulse-momentum relationships, using the coefficient of restitution. Pant and Wijeywickrema [13] have presented the three-dimensional (3D) simulation of seismic pounding between reinforced concrete (RC) moment-resisting frame buildings considering material as well as geometric nonlinearities. Two recently proposed variations of the linear contact element model namely, modified Kelvin-Voigt (MKV) model and modified Kelvin (MK) model were also compared in the referred paper. Rojas and Anderson [14] have presented a case study of 18-storey steel building (moment resisting frames) of Los Angeles during recorded San Fernando (1971) and Northridge (1994) earthquakes. This steel building was collided against the adjacent RCC parking structures. Recently, nonlinear finite element analysis in time domain has been carried out by Jameel et al.,[15] for pounding of neighbouring structures having varying heights. To show the importance of avoiding pounding in structures the results obtained were compared with model having no pounding phenomena. The results were obtained in the form of storey shear, pounding force, storey drift, point displacement and acceleration. More realistic modeling such as beams, columns and slabs has been adopted to accurately understand the pounding phenomenon.

More recently, it was also reported by Matsagar & Jangid [16] that the impact plays a vital role in the response of base isolated structures for the design of base isolation devices which strike against the earth retaining wall. Since base isolation is relatively a new technique, pounding phenomenon in base isolated buildings has been adequately investigated now a days. This type of study was carried out by Agarwal et al. [17] for the base isolated response of adjacent two story building systems. A specialized software has been developed by Komodromos et al. [18] in order to perform numerical simulations and parametric investigation efficiently on seismic pounding. The numerical simulations presented in the referred paper have exposed that even if a sufficient gap is provided at the base against moat wall by which pounding could be avoided. But this does not ensure that the building will not eventually collide with neighboring buildings on the same platform due to the deformations of their superstructures. Shake table study on two multi-degree-of-freedom steel models was performed by Chau et al.,[19] to investigate the potential seismic poundings between two one storey adjacent buildings in Hong Kong.

During seismic pounding enormous amount of input energy is transferred or received from one structure to the adjoining structures, therefore the structural energy of pounding affected structure is much different than that of standalone structure with the absence of pounding incidences. Valles-Mottox and Reinhorn [20] introduced the concept of Pseudo Energy Radius (PER) to study the effect of pounding in buildings. The response of a SDOF system in the state space plane, subjected to seismic input was related to the elastic structural energy (Ee) of the system through the Pseudo Energy Radius. The Pseudo Energy Radius being expressed in unit of displacement could be used to determine the critical gap to preclude pounding (gcr) between adjacent structures. The stereomechanical approach has been used in the referred work to determine the post impact velocities of the colliding masses.

In spite of the fact that the research on earthquake-induced pounding between buildings

has been recently become sophisticated, the studies have often been conducted on much simplified structural models, considering linear and non-linear spring element for impact simulations. Mathematical modeling for pounding replication has been considerably developed in the recent years with the arrival of various powerful mathematical and structural tools but accuracy of result is highly unsure due to wide changes in the structural properties of impact elements. The numbers of idealization and assumptions have unavoidably been used in theoretical models of impact simulations. The minimum time step size is considered as 0.02 second to decide the response of pounding affected structures in the nonlinear time history analysis. Therefore, the main intention of the present work is to study the pounding influence of equal height adjacent structures with various available contact elements for impact simulation. The equation of motion for MDOF system for one side as well as both side pounding is being solved using a program especially prepared for this purpose using MATLAB package [21]. The impact response of fixed base multistoried reinforced concrete structures is investigated under different real earthquake ground motions. Few sets of solutions obtained from the program are also compared with SAP 2000 NL [22] software results. The specific objectives of the present study are

i) To investigate pounding force response of lumped MDOF models by considering the existing various contact element mechanism for impact simulations, and

ii) To compare the total structural energy absorption capacity of the MDOF models under pounding by considering various existing impact simulation techniques.

## 2. CONTACT ELEMENT MECHANISMS FOR IMPACT SIMULATIONS

Seismic pounding is essentially a problem of dynamic impact. The forces produced during collision act over a short period of time, where energy is dissipated as heat due to random molecular vibrations and the internal friction of the colliding bodies [5]. Usually, contact is modeled using either a continuous force model by using contact element approach or via a stereo-mechanical (coefficient of restitution) approach. The contact element approach has been widely used by the researchers because of its easy adaptableness and reasonable accuracy. The impact forces generated during the collision of two adjacent structures can readily be thought as being provided by a contact element, which is activated only when the structures come into contact. The collision forces are assumed to act in a continuous manner. The contact element is usually a spring of very high stiffness, which may be used in combination with a damping element. The high spring stiffness is necessary to provide a realistic estimate of the impact force, ensure small impact duration and limit the penetration or overlapping of the colliding structures. The contact element is linear or nonlinear based on the stiffness of spring element and the damping properties of dashpot. The stereomechanical model, which works on the principle of momentum conservation and coefficient of restitution, is rather not recommended when a precise pounding involved structural response is required especially in the case of multiple impacts with longer duration [23]. The stereomechanical approach uses the instantaneous impact for which the duration of impact should be very small, which is not possible in the case of building pounding. Furthermore, this approach cannot be easily programmed in widely used commercially available software [24].

Therefore, in the present work investigations are reported for the effect of contact elements on the impact response of the adjacent structures and are explained in the successive paragraph as well as a illustrative view of all these contact elements are given in Fig. 1.

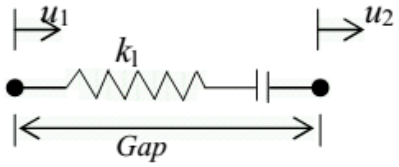


(a) Linear spring element

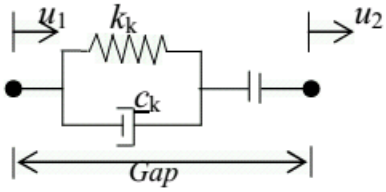


(b) Kelvin-Voigt element

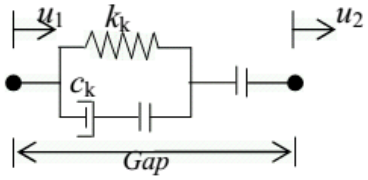


(c) Modified Kelvin-Voigt element

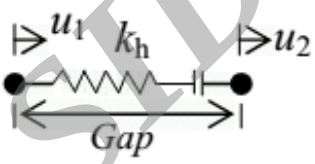


(d) Hertz contact element

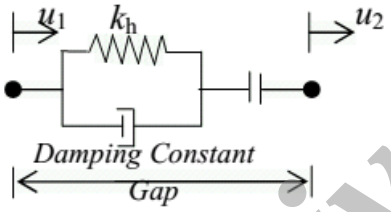


(e) Hertz-damp contact element

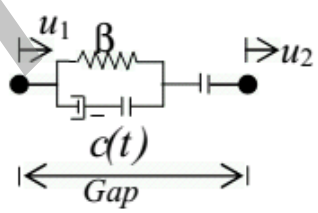


(f) Nonlinear viscoelastic element

Figure 1. Contact elements for impact simulation

*2.1 Linear spring contact element*

A linear impact of stiffness ($k_l$) can be used to simulate impact once the gap between adjacent structures closes. The impact force at time t is provided by

$$F_c(t) = k_1\delta(t), \tag{1}$$

Where, $\delta(t)$ is the interpenetration depth of the colliding bodies. This approach is relatively straightforward and can be easily implemented in commercial software. However, in the formulation the energy loss during impact is not taken into account. This model is shown in Fig. 1(a) which has been extensively used for impact simulation by Maison and Kasai [9].

*2.2 Kelvin-Voigt element contact element*

A linear impact spring of stiffness ($k_k$) is used to be in conjunction with a damper element ($c_k$) that accounts for energy dissipation during impact. The model shown in Fig. 1(b) has been widely used in some studies reported by Anagnostopoulos [4]. The impact force penetration relation can be represented as

$$F_c(t) = k_k \delta(t) + c_k \dot{\delta}(t) \quad (2)$$

Where, $\dot{\delta}(t)$ is the relative velocity between the colliding bodies at time t. the damping coefficient $c_k$ can be related to the coefficient of restitution e, by equating the energy losses during impact:

$$c_k = 2\xi\sqrt{k_k\left(\frac{m_1 m_2}{m_1 + m_2}\right)} \quad (3)$$

$$\xi = -\frac{\ln e}{\sqrt{\pi^2 + (\ln e)^2}} \quad (4)$$

The damping force in the Kelvin-Voigt model causes negative impact forces that pull the colliding bodies together, during the unloading phase, instead of pushing them apart. To avoid the tensile impact forces, slight modification is proposed by Komodromos et al,[18]. The modified equation for the next time interval is written as

$$F_c(t+\Delta t) = \begin{cases} k_k\delta(t) + c_k\dot{\delta}(t) & F_c(t) > 0, \\ 0 & F_c(t) \le 0. \end{cases} \quad (5)$$

*2.3 The modified kelvin-voigt contact element*

This model is developed by Pant and Wijeywickrema [13]. Here, the impact force $F_c(t)$ is expressed as,

$$F_c(t+\Delta t) = \begin{cases} k_k\delta(t) + c_k\dot{\delta}(t) & \delta > 0 \text{ and } \dot{\delta} > 0, \\ k_k\delta(t) & \delta > 0 \text{ and } \dot{\delta} \le 0, \\ 0 & \delta \le 0 \end{cases} \quad (6)$$

Where, $k_k$ is the stiffness of spring element, $c_k$ is the damping coefficient, indentation at contact surface is $\delta$ and relative velocity of impact is $\dot{\delta}$.

$$c_k = \xi\delta \text{ and } \xi = \frac{3k_k(1-e^2)}{2r^2\dot{\delta}_0} \quad (7)$$

Where, $\xi$ is damping ratio. In expression, e is the coefficient of restitution and $\dot{\delta}_0$ is the relative velocity just before the impact. This model is depicted in Fig. 1(c).

*2.4 Hertz contact element*

In pounding, it is expect that the contact area between neighboring structures should be increased as the contact force grows, leading to a non-linear stiffness. In order to model highly non-linear pounding more-realistically, Hertz impact model has been adopted by various researchers [7,19]. This model uses the Hertz contact law: a non-linear spring in an

impact oscillator.

The force in the contact element as shown in Fig. 1(d) can be expressed as:

$$F_c = \begin{cases} k_h \delta(t)^{3/2} & \delta(t) > 0, \\ 0 & \delta(t) \le 0. \end{cases} \tag{8}$$

Where, $\delta(t)$ is the relative displacement. Assuming that the colliding structures are spherical of density $\rho$ and the radius $R_i$ estimation can be calculated as:

$$R_i = \sqrt{\frac{3m_i}{4\pi\rho}}, \qquad i = 1,2 \tag{9}$$

The nonlinear spring stiffness $k_h$ is linked to the material properties and the radii of the colliding structures as stated through the equation 10 and 11:

$$k_h = \frac{4}{3\pi(h_1 + h_2)} \left[ \frac{R_1 R_2}{R_1 + R_2} \right]^{1/2} \tag{10}$$

Where, $h_1$ and $h_2$ are the material parameters defined by the Eqn 11:

$$h_i = \frac{1 - \gamma_i}{\pi E_i} \quad i = 1,2 \tag{11}$$

Here, $\gamma_i$ and $E_i$ are the Poisson's ratio and Young's Modulus respectively. The coefficient $k_h$ depends on material properties and geometry of colliding bodies. The Hertz contact law, is incapable of taking into account energy dissipation during impact phenomenon.

*2.5 Hertz damp contact element model*

An improved version of the Hertz model, called Hertzdamp model, has been considered by Muthukumar and DesRoches [25], wherein a non-linear damper is used in combination with the Hertz spring.

The pounding force for the model shown in Fig. 1(e) is written as

$$F(t) = k_h \delta^{3/2}(t) \left[ 1 + \frac{3(1 - e^2)}{4(v_1 - v_2)} \dot{\delta}(t) \right]; \ \delta(t) > 0 \ F(t) = 0; \ \delta(t) \le 0 \tag{12}$$

Where, e is the coefficient of restitution and $\dot{\delta}(t)$ is the relative velocity during contact and $v_1 - v_2$ is the relative approaching velocities prior to contact.

*2.6 Nonlinear viscoelastic model*

Another improved version of the Hertz model has been introduced by Jankowski [26] as shown in Fig. 1(f) by connecting a nonlinear damper in unison with the nonlinear spring.

The contact force for this model is expressed as:

$$\begin{aligned} F(t) &= \beta\delta(t)^{3/2} + \bar{c}(t)\dot{\delta}(t);\ \ \delta(t) > 0 \text{ and } \dot{\delta}(t) > 0 \text{ (Approach period)} \\ F(t) &= \beta\delta(t)^{3/2};\ \delta(t) > 0 \text{ and } \dot{\delta}(t) < 0 \text{ (restitution period)} \\ F(t) &= 0;\ \delta(t) \le 0 \end{aligned} \tag{13}$$

Where, β is the impact stiffness parameter and $\bar{c}(t)$ is the impact element damping. Here $\xi$ is an impact damping ratio corresponding to a coefficient of restitution e which can be defined as;

$$\begin{aligned} \xi &= \frac{9\sqrt{5}}{2}\frac{1-e^2}{e(e(9\pi-16)+16)} \\ \bar{c}(t) &= 2\xi\sqrt{\beta\sqrt{\delta(t)}\frac{m_1 m_2}{m_1+m_2}} \end{aligned} \tag{14}$$

In addition to the above contact element models, recently various contact element models have been added in the pounding simulation contact element dictionary by the researchers from all around the globe [8,27,28]. But those were not going to be considered in the present study.

## 3. MATHEMATICAL FORMULATIONS AND COMPUTATIONAL CONSIDERATIONS

The theoretical formulation for modeling of adjacent fixed base three degree of freedom structure is presented in this section. Originally, this formulation for fixed base building subjected to earthquake excitation was presented by Anagnostopoulos [4]. Fig. 2 gives an idea about the lumped masses at each floor, storey-wise stiffness and linear viscous dashpot constants of each building in detail. It also shows the gap element stiffness, separation distance and damping constant between the adjacent structures.

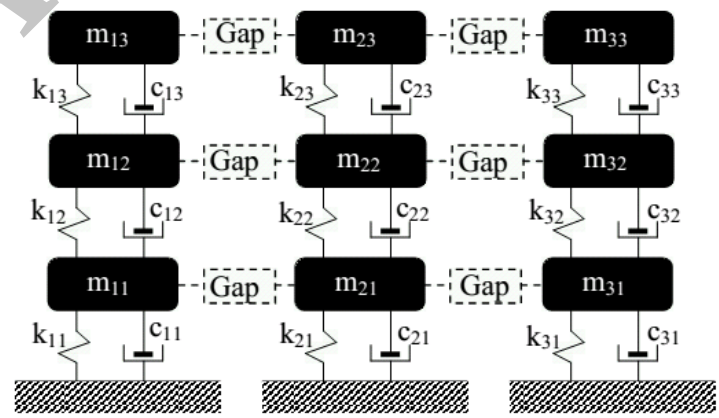


Figure 2. MDOF lumped mass system

Dynamic equations for the pounding between multi degree of freedom systems can be written by drawing the free body diagrams for the lumped masses and then by using equilibrium equations. These equations can be more conveniently expressed in the matrix form as mentioned in respective sections.

$$
\begin{bmatrix}
m_{11} & 0 & 0 & 0 & 0 & 0 & 0 & 0 & 0 \\
0 & m_{12} & 0 & 0 & 0 & 0 & 0 & 0 & 0 \\
0 & 0 & m_{13} & 0 & 0 & 0 & 0 & 0 & 0 \\
0 & 0 & 0 & m_{21} & 0 & 0 & 0 & 0 & 0 \\
0 & 0 & 0 & 0 & m_{22} & 0 & 0 & 0 & 0 \\
0 & 0 & 0 & 0 & 0 & m_{23} & 0 & 0 & 0 \\
0 & 0 & 0 & 0 & 0 & 0 & m_{31} & 0 & 0 \\
0 & 0 & 0 & 0 & 0 & 0 & 0 & m_{32} & 0 \\
0 & 0 & 0 & 0 & 0 & 0 & 0 & 0 & m_{33}
\end{bmatrix}
\begin{Bmatrix}
\ddot{x}_{11} \\ \ddot{x}_{12} \\ \ddot{x}_{13} \\ \ddot{x}_{21} \\ \ddot{x}_{22} \\ \ddot{x}_{23} \\ \ddot{x}_{31} \\ \ddot{x}_{32} \\ \ddot{x}_{33}
\end{Bmatrix} +
$$

$$
\left(
\begin{bmatrix}
c_{11}+c_{12} & -c_{12} & 0 & 0 & 0 & 0 & 0 & 0 & 0 \\
-c_{12} & c_{12}+c_{13} & -c_{13} & 0 & 0 & 0 & 0 & 0 & 0 \\
0 & -c_{13} & c_{13} & 0 & 0 & 0 & 0 & 0 & 0 \\
0 & 0 & 0 & c_{21}+c_{22} & -c_{22} & 0 & 0 & 0 & 0 \\
0 & 0 & 0 & -c_{22} & c_{22}+c_{23} & -c_{23} & 0 & 0 & 0 \\
0 & 0 & 0 & 0 & -c_{23} & c_{23} & 0 & 0 & 0 \\
0 & 0 & 0 & 0 & 0 & 0 & c_{31}+c_{32} & -c_{32} & 0 \\
0 & 0 & 0 & 0 & 0 & 0 & -c_{32} & c_{32}+c_{33} & -c_{33} \\
0 & 0 & 0 & 0 & 0 & 0 & 0 & -c_{33} & c_{33}
\end{bmatrix} +
\begin{bmatrix}
c_{1121} & 0 & 0 & -c_{1121} & 0 & 0 & 0 & 0 & 0 \\
0 & c_{1222} & 0 & 0 & -c_{1222} & 0 & 0 & 0 & 0 \\
0 & 0 & c_{1323} & 0 & 0 & -c_{1323} & 0 & 0 & 0 \\
-c_{1121} & 0 & 0 & c_{1121}+c_{2131} & 0 & 0 & -c_{2131} & 0 & 0 \\
0 & -c_{1222} & 0 & 0 & c_{1222}+c_{2232} & 0 & 0 & -c_{2232} & 0 \\
0 & 0 & -c_{1323} & 0 & 0 & c_{1323}+c_{2333} & 0 & 0 & -c_{2333} \\
0 & 0 & 0 & -c_{2131} & 0 & 0 & c_{2131} & 0 & 0 \\
0 & 0 & 0 & 0 & -c_{2232} & 0 & 0 & c_{2232} & 0 \\
0 & 0 & 0 & 0 & 0 & -c_{2333} & 0 & 0 & c_{2333}
\end{bmatrix}
\right)
\begin{Bmatrix}
\dot{x}_{11} \\ \dot{x}_{12} \\ \dot{x}_{13} \\ \dot{x}_{21} \\ \dot{x}_{22} \\ \dot{x}_{23} \\ \dot{x}_{31} \\ \dot{x}_{32} \\ \dot{x}_{33}
\end{Bmatrix}
$$

$$
+
\left(
\begin{bmatrix}
k_{11}+k_{12} & -k_{12} & 0 & 0 & 0 & 0 & 0 & 0 & 0 \\
-k_{12} & k_{12}+c_{13} & -k_{13} & 0 & 0 & 0 & 0 & 0 & 0 \\
0 & -k_{13} & k_{13} & 0 & 0 & 0 & 0 & 0 & 0 \\
0 & 0 & 0 & k_{21}+k_{22} & -k_{22} & 0 & 0 & 0 & 0 \\
0 & 0 & 0 & -k_{22} & k_{22}+k_{23} & -c_{23} & 0 & 0 & 0 \\
0 & 0 & 0 & 0 & -k_{23} & k_{23} & 0 & 0 & 0 \\
0 & 0 & 0 & 0 & 0 & 0 & k_{31}+k_{32} & -k_{32} & 0 \\
0 & 0 & 0 & 0 & 0 & 0 & -k_{32} & k_{32}+k_{33} & -k_{33} \\
0 & 0 & 0 & 0 & 0 & 0 & 0 & -k_{33} & k_{33}
\end{bmatrix} +
\begin{bmatrix}
s_{1121} & 0 & 0 & -s_{1121} & 0 & 0 & 0 & 0 & 0 \\
0 & s_{1222} & 0 & 0 & -s_{1222} & 0 & 0 & 0 & 0 \\
0 & 0 & s_{1323} & 0 & 0 & -s_{1323} & 0 & 0 & 0 \\
-s_{1121} & 0 & 0 & s_{1121}+s_{2131} & 0 & 0 & -c_{2131} & 0 & 0 \\
0 & -s_{1222} & 0 & 0 & s_{1222}+s_{2232} & 0 & 0 & -s_{2232} & 0 \\
0 & 0 & -s_{1323} & 0 & 0 & s_{1323}+s_{2333} & 0 & 0 & -s_{2333} \\
0 & 0 & 0 & -s_{2131} & 0 & 0 & s_{2131} & 0 & 0 \\
0 & 0 & 0 & 0 & -s_{2232} & 0 & 0 & s_{2232} & 0 \\
0 & 0 & 0 & 0 & 0 & -s_{2333} & 0 & 0 & s_{2333}
\end{bmatrix}
\right)
\begin{Bmatrix}
x_{11} \\ x_{12} \\ x_{13} \\ x_{21} \\ x_{22} \\ x_{23} \\ x_{31} \\ x_{32} \\ x_{33}
\end{Bmatrix}
\tag{15}
$$

$$
\begin{bmatrix}
-s_{1121}d_{1121} \\
-s_{1121}d_{1121} \\
-s_{1121}d_{1121} \\
s_{1121}d_{1121}-s_{2131}d_{2131} \\
s_{1222}d_{1222}-s_{2232}d_{2131} \\
s_{1323}d_{1323}-s_{2333}d_{2131} \\
s_{2131}d_{2131} \\
s_{2232}d_{2131} \\
s_{2333}d_{2131}
\end{bmatrix}
= -
\begin{bmatrix}
m_{11} & 0 & 0 & 0 & 0 & 0 & 0 & 0 & 0 \\
0 & m_{12} & 0 & 0 & 0 & 0 & 0 & 0 & 0 \\
0 & 0 & m_{13} & 0 & 0 & 0 & 0 & 0 & 0 \\
0 & 0 & 0 & m_{21} & 0 & 0 & 0 & 0 & 0 \\
0 & 0 & 0 & 0 & m_{22} & 0 & 0 & 0 & 0 \\
0 & 0 & 0 & 0 & 0 & m_{23} & 0 & 0 & 0 \\
0 & 0 & 0 & 0 & 0 & 0 & m_{31} & 0 & 0 \\
0 & 0 & 0 & 0 & 0 & 0 & 0 & m_{32} & 0 \\
0 & 0 & 0 & 0 & 0 & 0 & 0 & 0 & m_{33}
\end{bmatrix}
\begin{Bmatrix}
\ddot{x}_g \\ \ddot{x}_g \\ \ddot{x}_g \\ \ddot{x}_g \\ \ddot{x}_g \\ \ddot{x}_g \\ \ddot{x}_g \\ \ddot{x}_g \\ \ddot{x}_g
\end{Bmatrix}
$$

Where, $m_{11}$, $m_{12,}$ $m_{13}$ are the lumped masses at first, second and third storey of left building respectively. The first subscript indicates the structure number (i.e. 1 for left, 2 for middle and 3 for right structure) and second subscript denotes the storey number from bottom. Similarly, the storey stiffness and damping properties of the structure are considered.

$s_{1121}$ and $c_{1121}$ are the gap element stiffness and damping properties used between the interaction of left and middle structures at the first storey level masses, respectively, the first and third subscripts denotes the structural number (i.e. 1 for left, 2 for middle and 3 for right structure), wheareas second and fourth subscript indicates the storey level measured from bottom towards top. And so the other symbols for second and third storey level masses are defined s and used in the equations for all these structures. $d_{1121}$ is the separation distance between the left and middle structures and $d_{2131}$ is the separation distance between the middle and right structures.

The Eqn 15 can be written in more general sense in matrix form for whole configuration as below.

$$[\mathrm{m}]\{\ddot{\mathrm{x}}\}+[\mathrm{c}]\{\dot{\mathrm{x}}\}+[\mathrm{k}]\{\mathrm{x}\}+\{\mathrm{k_s}\}=-[\mathrm{m}]\{\ddot{\mathrm{x}}_{\mathrm{g}}\} \tag{16}$$

Where, $\{x\}$ is the displacement vector for all degrees of freedom (DOF), $\{\dot{x}\}$ is the velocity vector associated to DOF, and $\{\ddot{x}\}$ is the acceleration vector associated to DOF. $[m]$ is the mass matrix, $[c]$ is the total damping matrix consists of structural damping of Rayleigh type for lumped system and viscous damping constant matrix for gap elements, $[k]$ is the total stiffness matrix combination of elastic stiffness matrix of structure as well as the gap elements stiffness matrix. $\{k_s\}$ is the spare constant gap element stiffness matrix, and $\{\ddot{x}_g\}$ is the input ground acceleration.

A program is prepared in MATLAB for the three fixed base adjacent MDOF structures subjected to pounding, wherein the resulting system of second order equation is recast as a system of first order ordinary differential equations and then solved by using 'ode45' solvers in MATLAB. It was reported that 'ode45' solver can easily solve ordinary differential equation of structure and the results reasonably compare with the solution of new mark-Beta step by step integration method [17]. In the entire analysis, buildings are modeled as shear buildings which have the same height for floor collision and do not include frame behavior (considering floor as a rigid diaphragm). Inelastic behavior and any rotation of the buildings are also neglected. All systems are subjected to the same ground acceleration, which implies that any effects of phase difference due to travelling waves are also neglected.

## 4. ENERGY TRANSFERRED DURING POUNDING INTERACTION

When collision occurs during structural pounding, an interactive force between the two structures can be obtained as explained through equations 17 to 21, [20]. Consider the equation of motion of two SDOF structures, which are subjected to pounding.

$$m_1\ddot{u}_1 + c_1\dot{u}_1 + k_1u_1 + k_s = -m_1\ddot{x}_g \quad (17)$$

$$m_2\ddot{u}_2 + c_2\dot{u}_2 + k_2u_2 - k_s = -m_2\ddot{x}_g \quad (18)$$

Where, $u_1$, $\dot{u}_1$, $\ddot{u}_1$ are the displacement, velocity and acceleration of structure 1, respectively, similarly $u_2$, $\dot{u}_2$, $\ddot{u}_2$ are the displacement, velocity and acceleration of structure 2, respectively. $\ddot{x}_g$ is the ground acceleration; and $k_s$ is spare constant gap element force at the time of pounding.

The presence of interactive force during pounding in structures changes the energy balance in the structure, which leads to increase or decrease in the response. The equations for energy in structure 1 and 2 can be obtained from the respective equation of motion after multiplying it by corresponding velocities and integration over time on both sides. The energy equations are the relative energy equations.

$$E_{K1} + E_{\xi 1} + E_{P1} + E_{Tr12} = E_{I1} \quad (19)$$

$$E_{K2} + E_{\xi 2} + E_{P2} + E_{Tr21} = E_{I2} \quad (20)$$

Where, $E_I$ is the input energy; $E_K$ is the kinetic energy; $E_P$ is the potential deformation energy; and $E_\xi$ viscous damping energy for the structures and these are obtained as:

$$E_{K1} = \frac{m_1}{2}(\dot{u}_1)^2;\ E_{\xi 1} = \int_0^t c_1(\dot{u}_1)^2 d\tau;\ E_{P1} = \frac{k_1}{2}(u_1)^2;\ E_{I1} = -m_1\int_0^t \ddot{x}_g\dot{u}_1 d\tau \quad (21)$$

Similarly, it can be calculated for structure 2. The energy transfer from structure 1 to structure 2 is denoted by $E_{Tr12}$. Care should be taken that the energy transfer terms can be negative, since they are direction dependent. That is, a positive energy transfer term indicates that part of the input energy gets transferred to the adjoining structures, while negative energy transfer terms indicate that energy is received from other structures. Transfer energy ($E_{Tr}$) at each increment of time can be obtained after deducting the total structural energy ($E_S = E_K + E_\xi + E_P$) from the input energy ($E_I$).

## 5. ANALYTICAL STUDY

The numerical study presented in this paper is focused on pounding between three adjacent fixed base linear elastic multi-degree-of-freedom lumped mass models by using various contact element mechanisms for the impact simulation. In the aforesaid study, the left and right exterior structure is subjected to one side pounding whereas the middle structure undergoes both side pounding incidences. The results of MATLAB program for analysis of MDOF structure are verified under SAP 2000 NL software. In the present work, the three dimensional rectangular plan configuration structures have been selected for the study. For a simplistic analysis these 3-D structures are being converted into MDOF stick models by calculating the mass and stiffness properties at each storey levels as per the basic rules of structural dynamics. The MATLAB program considering different impact simulation

techniques have been prepared for stick model only, which are capable to work out the impact forces at the collision levels.

MDOF stick models which are chosen for the studies are mentioned as.

a) Model I - With a linear spring element for impact simulation.
b) Model II - With a Kelvin-Voigt element model for impact simulation
c) Model III - With a modified Kelvin-Voigt element for impact simulation
d) Model IV – With a Hertz contact element for impact simulation
e) Model V – With a Hertz-damp contact element for impact simulation
f) Model VI – With a nonlinear viscoelastic contact element for impact simulation.
g) Model VII – With no pounding, structures act as a standalone structures.

The three nearby 3D structure selected for the present study are as shown in Fig. 3.

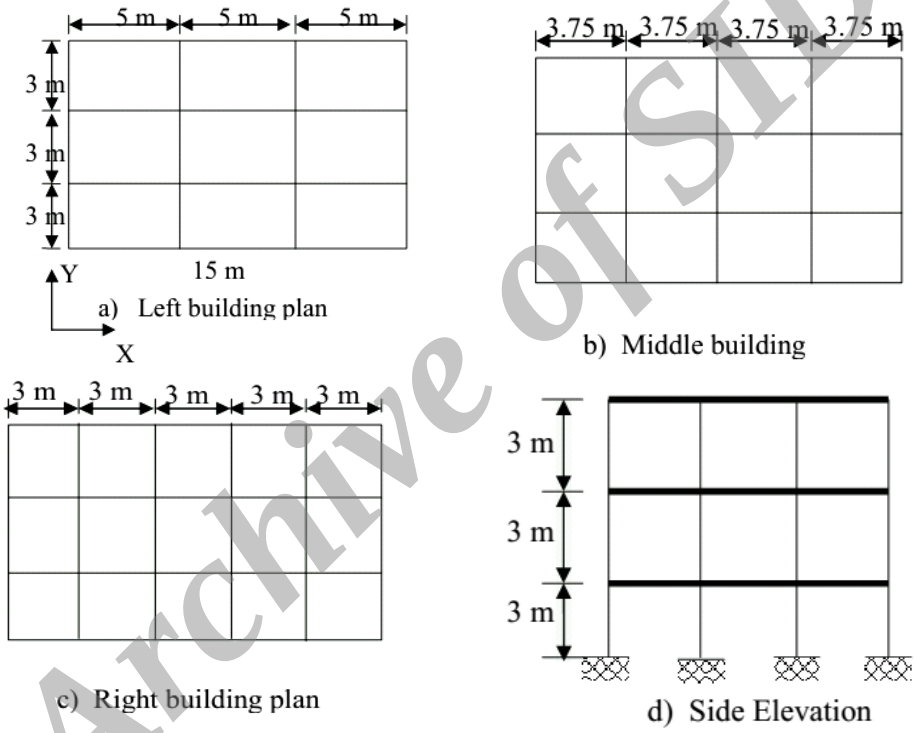


Figure 3. Three dimensional R.C.C. structure

The plan area of these three dimensional buildings are kept constant as 15 x 9 m. The structural and material properties of buildings are chosen randomly for the present work. The M25 grade of concrete is considered and modulus of elasticity is calculated as per the formulation given in IS 456:2000 code (Ec = $5000\sqrt{f_{ck}}$). The beam and column sizes in each building are considered constant at all storey levels. The wall is placed only over the outer beams. The other structural properties are mentioned in Table 1. Imposed load over the beams have considered as 4.5 kN/m$^2$. For seismic weight calculations 50 % contribution of imposed load is used in the study except for roof, where it has considered as zero. The full wall load is taken into account at all the floors including roof for the seismic weight calculations.

Table 1: Structural properties for 3-D structures

| Description | Left Building | Middle Building | Right Building |
|---|---|---|---|
| Beam sizes | 0.23 x 0.45 m | 0.23 x 0.45 m | 0.23 x 0.45 m |
| Column sizes | 0.3 x 0.5 m | 0.3 x 0.4 m | 0.35 x 0.35 m |
| Slab thickness | 0.12 m | 0.12 m | 0.12 m |
| Wall Thickness | 0.23 m | 0.23 m | 0.23 m |

The three degree of freedom stick model (as shown in Fig. 2) is being prepared from 3-D structures. The lumped masses at each floor levels and storey stiffness are computed as per the principles of structural dynamics. The structural properties of MDOF stick models and gap element properties are mentioned in the respective sections below.

*5.1 Structural Properties for MDOF stick models*

$m_{11} = m_{21} = 173.331$ ton, $m_{31} = 133.956$ ton, $k_{11} = k_{21} = k_{31} = 555.55 \times 10^3$ kN/m, $m_{12} = m_{22} = 175.661$ ton, $m_{32} = 136.286$ ton, $k_{12} = k_{22} = k_{32} = 355.55 \times 10^3$ kN/m, $m_{13} = m_{23} = 182.041$ ton, $m_{33} = 140.641$ ton, $k_{13} = k_{23} = k_{33} = 333.472 \times 10^3$ kN/m, Rayleigh mass and stiffness proportional damping is being used for calculating the damping constants, wherein damping ratio for the first two modes have considered as 5 percent critical.

Where, $m_{11}$, $m_{21}$ and $m_{31}$ is the mass at storey level 1, 2 and roof level of left building, similarly $k_{11}$, $k_{21}$ and $k_{31}$ is the stiffness of storey 1, 2 and 3 of left building. In the same manner the mass and stiffnesses of middle and right structures are denoted and as given in Fig. 2.

*5.2 Gap element properties for MDOF stick models*

The contact element approach has its limitation, with the exact value of spring stiffness to be used, being unclear. Uncertainty in the impact spring stiffness arises from the unknown geometry of impact surfaces, uncertain material properties under loading and variable impact velocities. The contact spring stiffness is typically taken as the in-plane axial stiffness of the colliding structure. Using a very high stiffness can lead to numerical convergence difficulties and unrealistically high impact forces, while a small stiffness can lead to more numbers of impacts with less magnitude impact forces. Therefore, the solution difficulty arises from the large changes in stiffness upon impact or contact loss, thus resulting in large unbalanced forces affecting the stability of the assembled equation of motion. Here, the value of gap element stiffness is calculated from the axial stiffness of rigid floor diaphragm as given in equation 22.

$$\text{Gap element stiffness for Model I, II \& III} = AE/L = 1.8 \times 10^6 \text{ kN/m.} \quad (22)$$

Where, A is the cross sectional area of rigid diaphragm (i.e. 9m x 0.12m), E is the Young's modulus of elasticity (i.e. $2.5 \times 10^7$ kN/m$^2$) and L is the length of diaphragm (i.e. 15 m).

The stiffness of gap element should be higher than the values obtained from equation 21, so from study point of view it is taken as $2 \times 10^6$ kN/m. In Model IV, V & VI the stiffness of gap element is calculated from equations 9, 10 & 11, respectively. In numerical investigations the value of coefficient of restitution for Model II, III, V & VI is adopted as

0.6, [26]. Separation distance between two successive MDOF adjoining structures have considered as 0.01 m for all storey levels. The Impact forces are calculated from the respective pounding force equation of each model as mentioned in sections 2.1 to 2.6.

Four real earthquake records have been incorporated in the analysis and their details are given in Table 2. All the records are taken from the PEER strong motion database (http://peer.berkeley.edu/smcat/). The characteristics of the recorded ground motions are exposed through the ground acceleration spectra (Refer Fig. 4). The output of time domain analysis of stick models have obtained in terms of displacements at the lumped mass locations, impact forces at the pounding levels and shear forces at all the storey levels for the entire duration of ground motion. In addition to this, output is also measured in terms of total structural energy and transferrable energy for all the stick models in the entire time domain analysis.

Table 2: Characteristics of real earthquakes used for the present study

| Captions of recorded ground motion | Year | Absolute acceleration component in terms of 'g' (9.81 m/s$^2$) | Duration (seconds) | Recorded station |
|---|---|---|---|---|
| Arleta, Northridge | 1994 | 0.344 | 40 | Arleta, CDMG 24087. |
| Santa Monica, Northridge | 1994 | 0.883 | 60 | Santa Monica, CDMG 24538 |
| El Centro | 1940 | 0.319 | 32 | Imperial Valley, USGS 117 |
| Sanfernando | 1971 | 1.16 | 41.82 | Pacoima Dam, CDMG 279, Component PCD 254 |

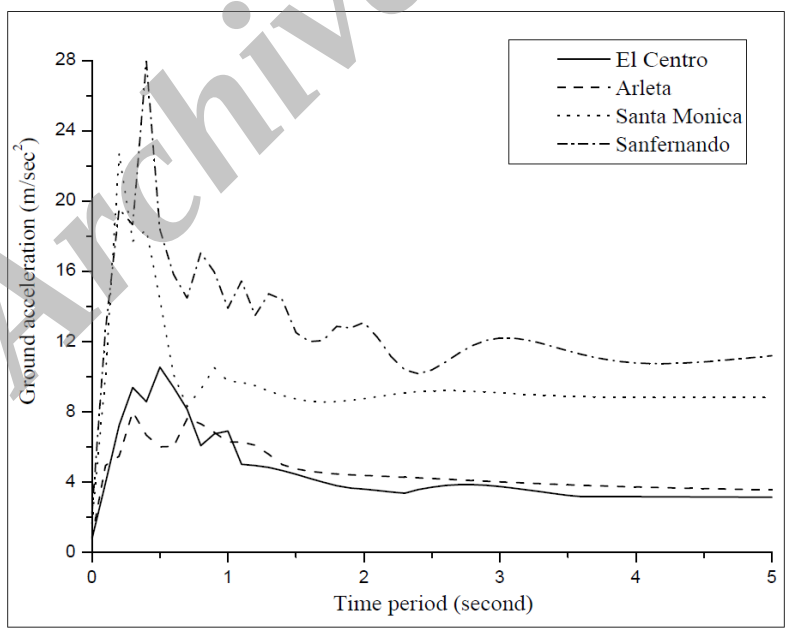


Figure 4. Ground acceleration spectra for 5 percent critical damping

## 6. RESULTS AND DISCUSSIONS

Analytical study of MDOF structure is carried out by considering seven models of impact simulation for three adjacent structures. Prior to actual numerical work, some validation study of the developed MATLAB program is also carried out and presented in the section below.

### *6.1 Validation of MATLAB program solution with SAP 2000 results*

Validation of prepared MATLAB code is being done for any one model, since for other models there have been minor changes in the gap element formulations. So here, the validation of MATLAB program is being done for Model I of section 5 by using SAP 2000 NL software results. For the stick models of three adjacent MDOF structure of Model I the structural and gap element properties are picked up from section 5 during modeling the structure in SAP 2000 software. SAP 2000 will have some limitations such as; it can model the adjacent buildings by using the linear spring gap element or by appropriate spring-dampers gap element in which the damping is constant throughout process of time integration. Thus, it is understood that SAP 2000 can model the structure for linear or Kelvin impact simulation techniques only. But apart from this limitation, it can very easily reproduce the results for Model I with reasonable degree of accuracy. So, in the present paper the Model I is considered for comparison of results.

Case I – Model I is analyzed using MATLAB program (MATLAB Model)

Case II – Model I is analyzed using SAP 2000 NL software (SAP Model)

The validation study of Model I have presented for the fixed base MDOF lumped mass model considering all the ground motions stated earlier. Displacement verification results of MATLAB and SAP is given in Table 3. The displacements of Table 3 are only the peak values in forth and back direction of motion. Whereas, Table 4 shows the peak impact force verification for the above two cases.

Table 3: Storey-wise peak displacement comparison between SAP and MATLAB (For this study only Model I is consider)

| Input ground motion | Storey level | Left structure | | | | Middle structure | | | | Right structure | | | |
|---|---|---|---|---|---|---|---|---|---|---|---|---|---|
| | | Forth direction | | Back direction | | Forth direction | | Back direction | | Forth direction | | Back direction | |
| | | SAP | Matlab | SAP | Matlab | SAP | Matlab | SAP | Matlab | SAP | Matlab | SAP | Matlab |
| El Centro | 1 | 0.004 | 0.004 | 0.005 | 0.005 | 0.008 | 0.008 | 0.009 | 0.009 | 0.005 | 0.004 | 0.006 | 0.004 |
| | 2 | 0.008 | 0.008 | 0.008 | 0.009 | 0.015 | 0.014 | 0.016 | 0.016 | 0.007 | 0.007 | 0.007 | 0.007 |
| | 3 | 0.009 | 0.009 | 0.010 | 0.010 | 0.018 | 0.017 | 0.018 | 0.02 | 0.010 | 0.009 | 0.010 | 0.009 |
| Arleta | 1 | 0.004 | 0.005 | 0.006 | 0.006 | 0.012 | 0.011 | 0.009 | 0.009 | 0.003 | 0.003 | 0.005 | 0.005 |
| | 2 | 0.011 | 0.010 | 0.009 | 0.010 | 0.018 | 0.020 | 0.015 | 0.017 | 0.007 | 0.006 | 0.010 | 0.009 |
| | 3 | 0.010 | 0.011 | 0.013 | 0.014 | 0.021 | 0.022 | 0.019 | 0.020 | 0.010 | 0.011 | 0.012 | 0.011 |
| Santa Monica | 1 | 0.012 | 0.012 | 0.013 | 0.014 | 0.021 | 0.022 | 0.018 | 0.020 | 0.015 | 0.014 | 0.012 | 0.011 |
| | 2 | 0.024 | 0.025 | 0.023 | 0.024 | 0.035 | 0.036 | 0.027 | 0.029 | 0.025 | 0.023 | 0.021 | 0.019 |
| | 3 | 0.032 | 0.034 | 0.029 | 0.030 | 0.042 | 0.043 | 0.034 | 0.036 | 0.040 | 0.038 | 0.027 | 0.025 |
| Sanfer nando | 1 | 0.014 | 0.012 | 0.012 | 0.013 | 0.019 | 0.021 | 0.018 | 0.019 | 0.010 | 0.012 | 0.011 | 0.012 |
| | 2 | 0.021 | 0.020 | 0.021 | 0.022 | 0.031 | 0.032 | 0.029 | 0.030 | 0.018 | 0.020 | 0.018 | 0.020 |
| | 3 | 0.024 | 0.023 | 0.025 | 0.027 | 0.039 | 0.041 | 0.034 | 0.036 | 0.032 | 0.033 | 0.020 | 0.022 |

(All displacements are in meters)

Table 4: Storey-wise impact force comparison between SAP and MATLAB (For this study only Model I is consider)

| Input ground motion | Storey levels | Between left & middle structures | | | | Between middle & right structures | | | |
|---|---|---|---|---|---|---|---|---|---|
| | | SAP | | Matlab | | SAP | | Matlab | |
| | | PIF* | $N^+$ | PIF* | $N^+$ | PIF* | $N^+$ | PIF* | $N^+$ |
| El Centro | 1 | 0 | 0 | 0 | 0 | 0 | 0 | 0 | 0 |
| | 2 | 940 | 6 | 925 | 7 | 803 | 3 | 795 | 3 |
| | 3 | 1198 | 16 | 1184 | 17 | 1177 | 8 | 1117 | 7 |
| Arleta | 1 | 0 | 0 | 0 | 0 | 0 | 0 | 0 | 0 |
| | 2 | 792 | 10 | 683 | 11 | 729 | 4 | 710 | 5 |
| | 3 | 1146 | 18 | 1192 | 16 | 1033 | 8 | 1013 | 9 |
| Santa Monica | 1 | 680 | 3 | 674 | 3 | 1510 | 8 | 1468 | 9 |
| | 2 | 2303 | 25 | 2292 | 28 | 3820 | 25 | 3779 | 27 |
| | 3 | 3090 | 42 | 3024 | 45 | 4192 | 34 | 4124 | 32 |
| Sanfernando | 1 | 666 | 12 | 652 | 13 | 1124 | 19 | 1080 | 21 |
| | 2 | 2205 | 54 | 2145 | 58 | 2112 | 58 | 2091 | 64 |
| | 3 | 2942 | 71 | 2906 | 74 | 3197 | 63 | 3158 | 66 |

*PIF** Peak impact force (kN)
$N^+$ Number of impacts

Validation of MATLAB solution is carried out prior to the comparative study as discussed in the subsequent sections. It is noted that the response of Model I obtained from SAP 2000 and also from MATLAB code are in good agreement. So for preliminary study of pounding in structures like plane frame structure and space frame structure where programming became complex and cumbersome, the SAP 2000 software provides good results of the seismic analysis with reasonable degree of accuracy.

*6.2 Comparative study of three adjacent lumped MDOF system for the various impact simulation techniques*

For this comparative study, as mentioned in section 4, the 3D multistoried structure is converted into a stick model. The results of MATLAB program for peak displacements and shear forces at all storey levels between the adjacent stick models under four real earthquake ground motions are incorporated in Figs. 5 to 10. Table 5 presents the peak values of impact forces and number of impacts between three relative neighboring structures under used real ground inputs. Figs. 11, 12 and 13 shows the total structural strain energy versus time plots for all the models of left, middle and right structures respectively. The structural strain energy is obtained after adding up the potential energy, damping energy and kinetic energy. This total accumulated structural energy, if it is deducted from the input ground energy then the interactive energy is obtained for the individual structures. This interactive energy may be positive or negative, positive sign indicates the transferred form of energy from one structure to other and negative sign indicates the received form of energy from other structures. Table 6 shows the transfer or received energies from one structure to others for all the models under used ground excitations.

Table 5: Peak values of impact force and number of impacts for adjoining stick models

| Input ground motion | Storey levels | Collision between | Model I | Model II | Model III | Model IV | Model V | Model VI |
|---|---|---|---|---|---|---|---|---|
| El Centro | 1 | Left-middle | 0 | 0 | 0 | 0 | 0 | 0 |
| | | Middle -right | 0 | 0 | 0 | 0 | 0 | 0 |
| | 2 | Left-middle | 925 (7) | 893 (6) | 858 (7) | 65 (8) | 0 | 0 |
| | | Middle -right | 795 (3) | 147 (2) | 693 (3) | 51 (3) | 0 | 0 |
| | 3 | Left-middle | 1184 (17) | 1169 (16) | 1146 (17) | 93 (16) | 0 | 0 |
| | | Middle -right | 1117 (7) | 751 (3) | 1058 (7) | 87 (8) | 0 | 0 |
| Arleta | 1 | Left-middle | 0 | 0 | 0 | 0 | 0 | 0 |
| | | Middle -right | 0 | 0 | 0 | 0 | 0 | 0 |
| | 2 | Left-middle | 683 (11) | 972 (11) | 853 (10) | 51 (9) | 0 | 0 |
| | | Middle -right | 710 (5) | 683 (6) | 630 (7) | 35 (6) | 0 | 0 |
| | 3 | Left-middle | 1192 (16) | 1372 (14) | 1184 (17) | 97 (16) | 0 | 0 |
| | | Middle -right | 1013 (9) | 996 (9) | 944 (8) | 62 (9) | 0 | 0 |
| Santa Monica | 1 | Left-middle | 674 (3) | 1383 (4) | 588 (4) | 33 (4) | 67 (2) | 38 (2) |
| | | Middle -right | 1468 (9) | 1147 (6) | 1407 (10) | 99 (9) | 88 (4) | 76 (3) |
| | 2 | Left-middle | 2292 (28) | 2689 (28) | 2059 (31) | 274 (25) | 371 (8) | 186 (9) |
| | | Middle -right | 3779 (27) | 2769 (24) | 3560 (30) | 397 (25) | 282 (8) | 235 (7) |
| | 3 | Left-middle | 3024 (45) | 3139 (40) | 2643 (46) | 395 (43) | 346 (9) | 259 (11) |
| | | Middle -right | 4124 (32) | 2959 (27) | 3762 (37) | 324 (31) | 277 (7) | 219 (7) |
| Sanfernando | 1 | Left-middle | 652 (13) | 622 (17) | 577 (14) | 33 (11) | 17 (3) | 9 (2) |
| | | Middle -right | 1080 (21) | 774 (12) | 1012 (14) | 59 (15) | 26 (4) | 40 (3) |
| | 2 | Left-middle | 2145 (58) | 1742 (46) | 1824 (58) | 216 (53) | 141 (22) | 132 (24) |
| | | Middle -right | 2091 (64) | 1925 (55) | 2223 (63) | 227 (58) | 177 (15) | 125 (17) |
| | 3 | Left-middle | 2906 (74) | 2383 (70) | 2481 (70) | 340 (72) | 229 (27) | 137 (28) |
| | | Middle -right | 3158 (66) | 2449 (60) | 3298 (63) | 359 (57) | 205 (21) | 471 (24) |

*The values in the bracket indicate the number of collisions occurs and impact force magnitudes are given in kN.

After assessing the Figs. 5, 6 and 7, it is observed that in all the models of impact simulation, very less difference in the peak values of displacements in back and forth directions of structures is observed. Inevitably the top storey level produces more displacement than the lower ones. In El Centro ground excitation, peak displacement results are almost same amongst all the models (nature-wise and magnitude-wise also), but in all other three considered excitations, the peak displacement values are much varies in wider band and can easily noticed through figures. Santa Monica and Sanfernando ground excitations produce higher values of peak displacements of structures than other two considered ground excitations. Extreme right structure suffers more displacements than any other due to the effect of series-end building pounding.

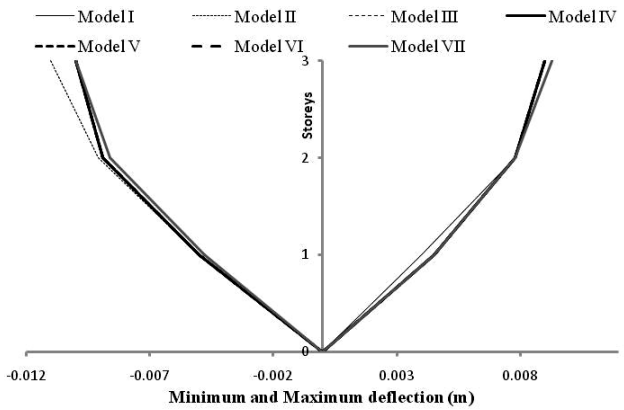


a) El Centro ground excitation

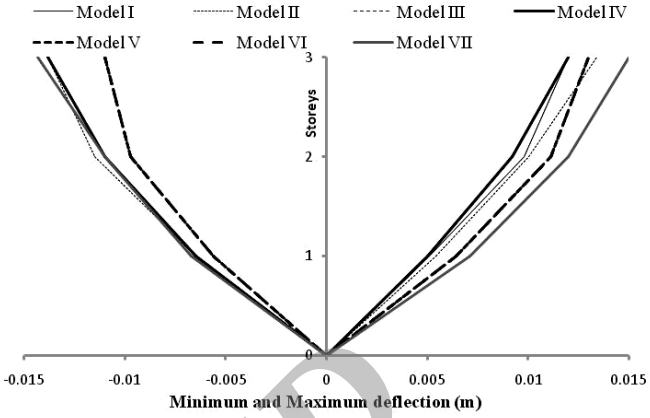


b) Arleta ground excitation

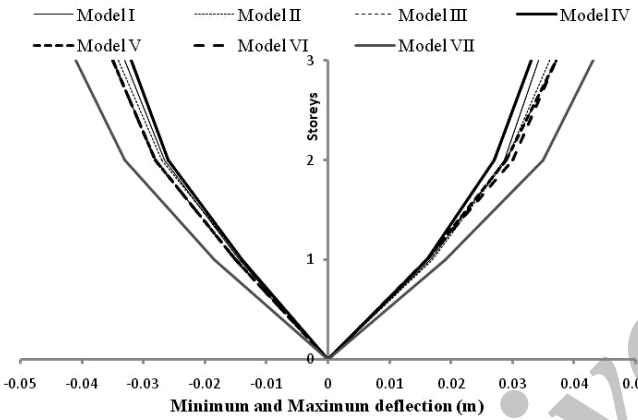


c) Santa Monica excitation

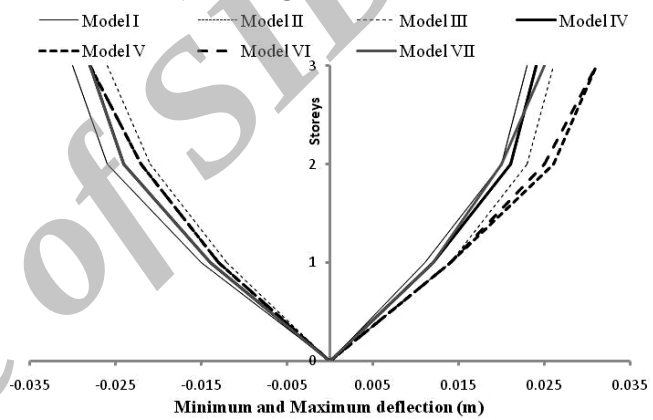


d) Sanfernando excitation

Figure 5. Storey-wise peak displacements of left structure

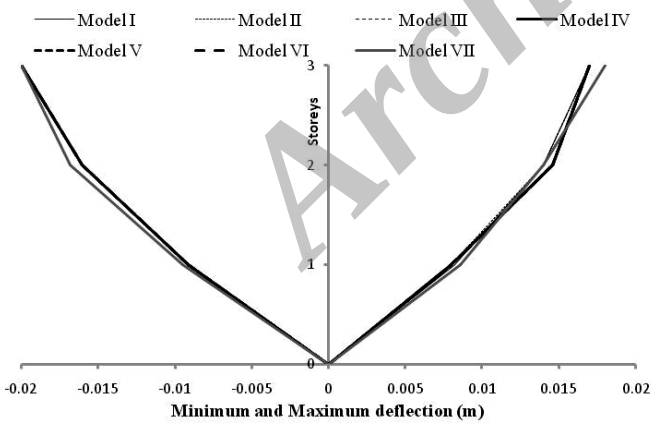


a) El Centro ground excitation

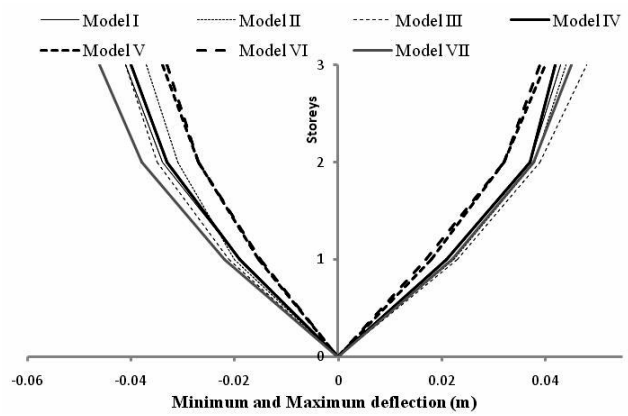


b) Arleta ground excitation

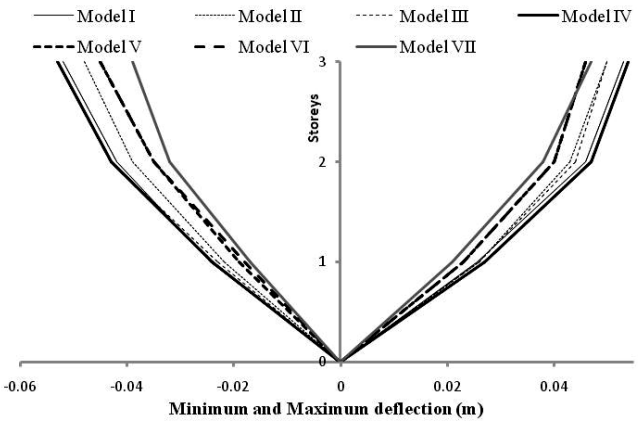


c) Santa Monica excitation

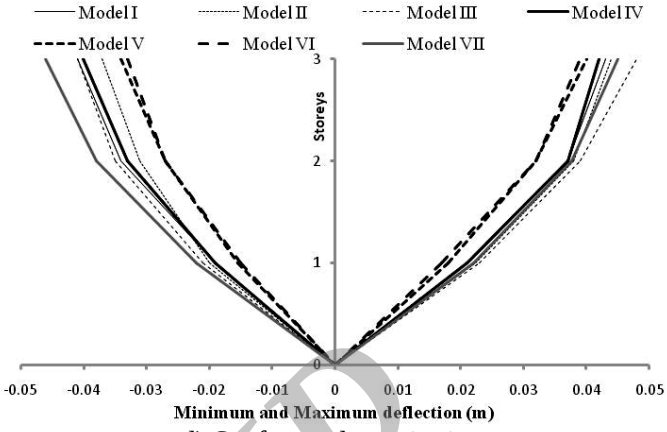


d) Sanfernando excitation

Figure 6. Storey-wise peak displacements of middle structure

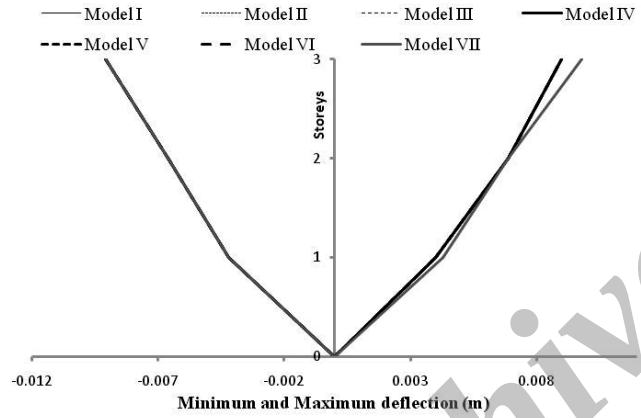


a) El Centro ground excitation

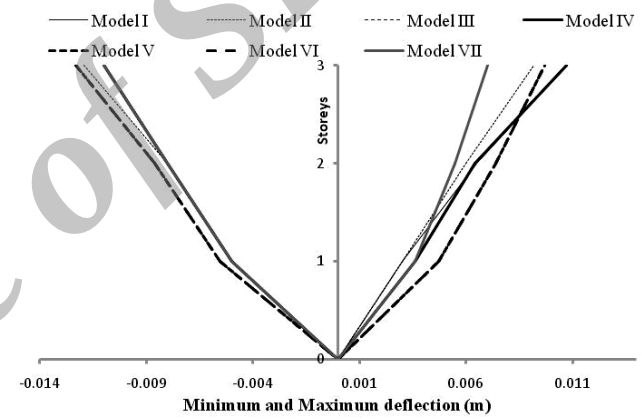


b) Arleta ground excitation

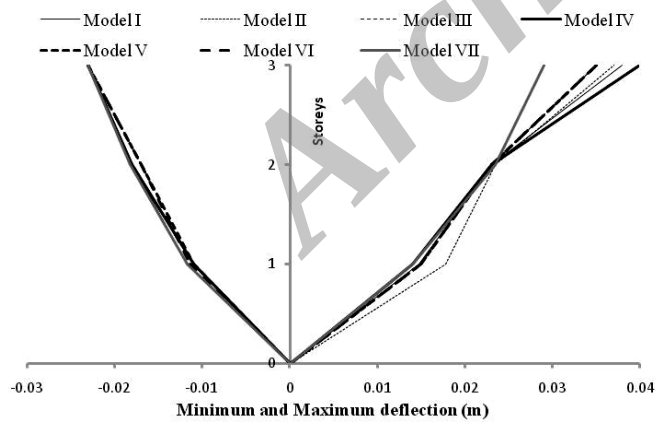


c) Santa Monica excitation

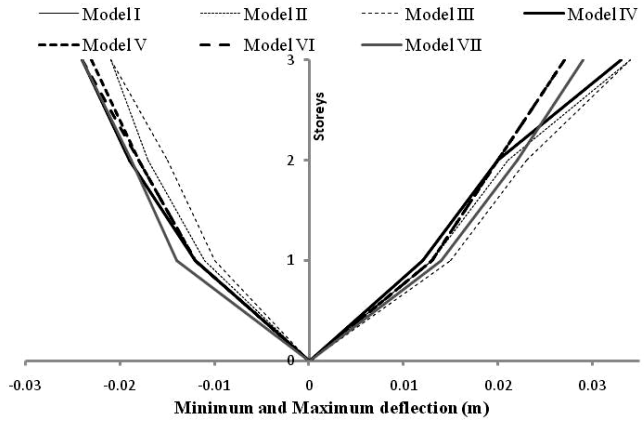


d) Sanfernando excitation

Figure 7. Storey-wise peak displacements of right structure

Figs. 8, 9 and 10, clearly shows that the impact forces during the instance of collision amplifies the shear forces in the side of pounding. In left and middle structures, the peak

values of shear forces are maximum at the base storey than the higher stories as expected, but in right structure, this pattern has not been seen that's because of the effect of end building pounding in a row. Santa Monica and Sanfernando excitation produce severe values of shear forces in the structures than the other two used excitations.

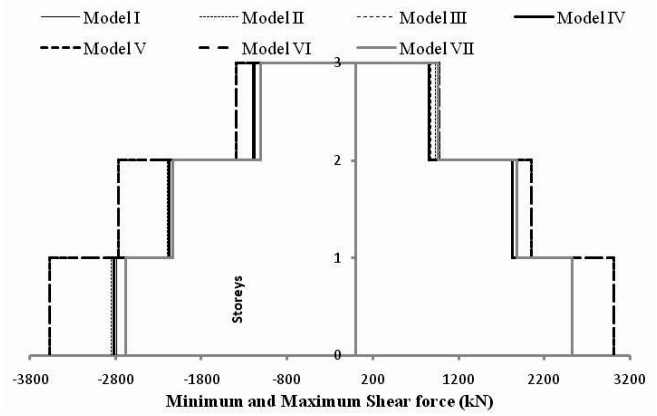


a) El Centro ground excitation

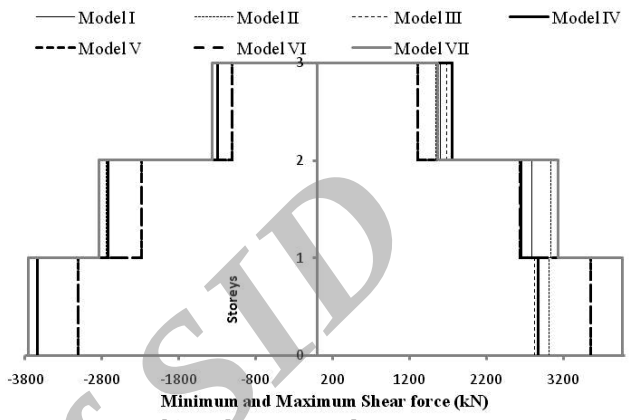


b) Arleta ground excitation

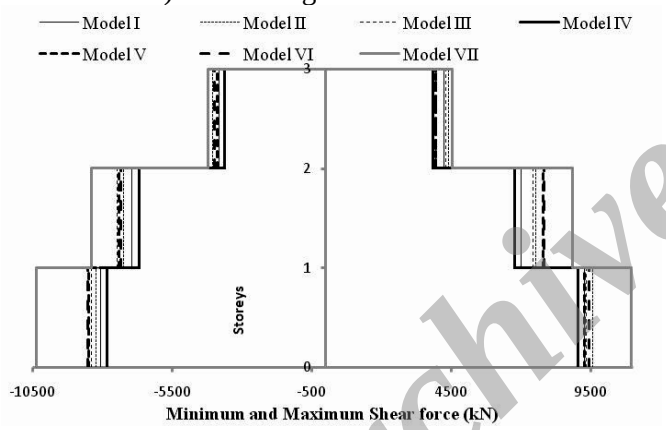


c) Santa Monica excitation

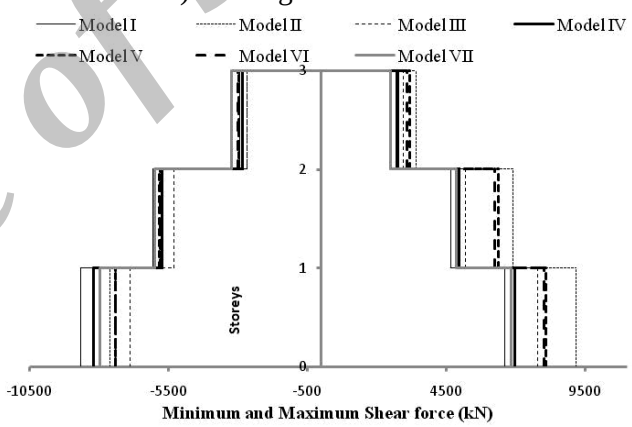


d) Sanfernando excitation

Figure 8. Storey-wise shear forces of left structure

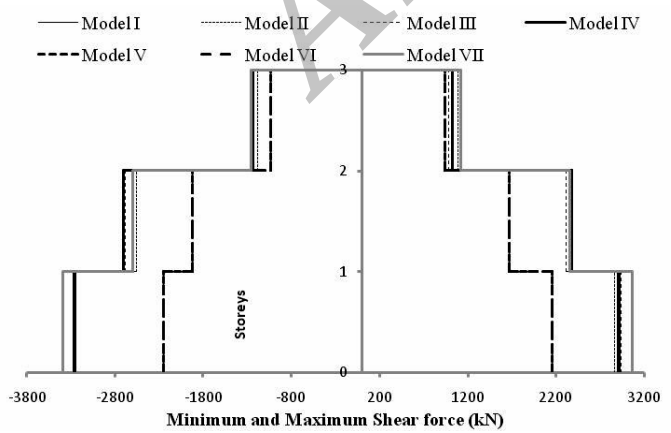


a) El Centro ground excitation

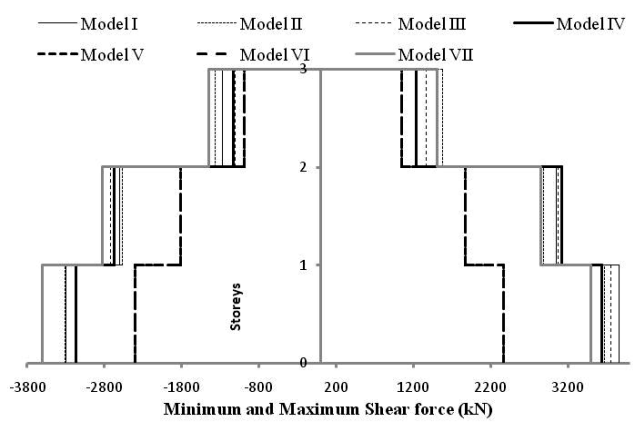


B) Arleta ground excitation

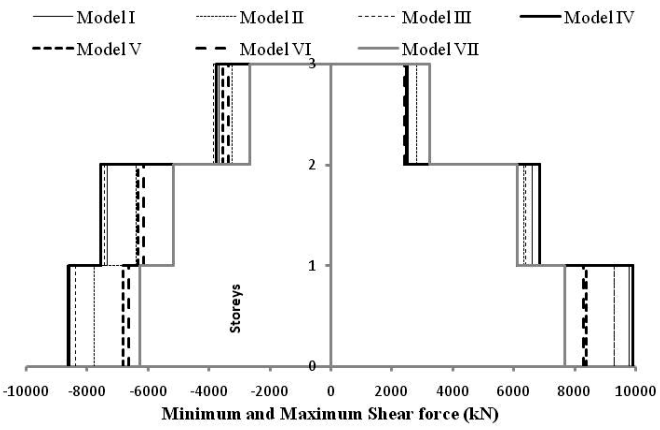


c) Santa Monica excitation

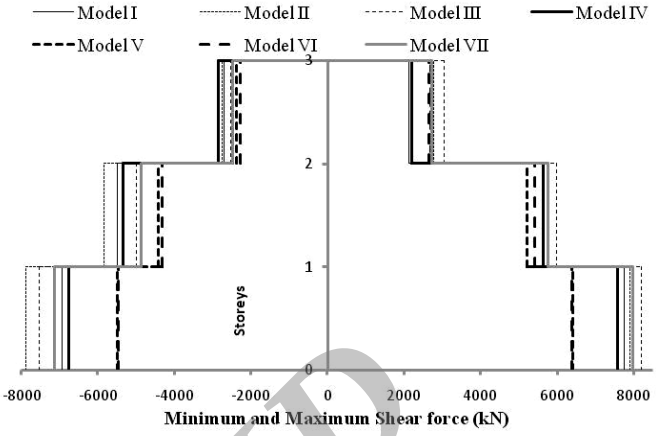


d) Sanfernando excitation

Figure 9. Storey-wise shear forces of middle structure

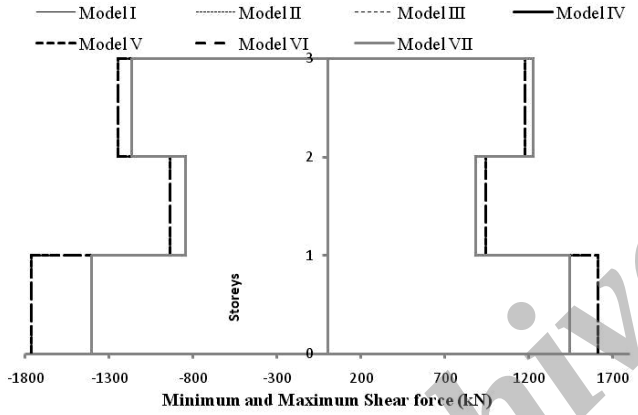


a) El Centro ground excitation

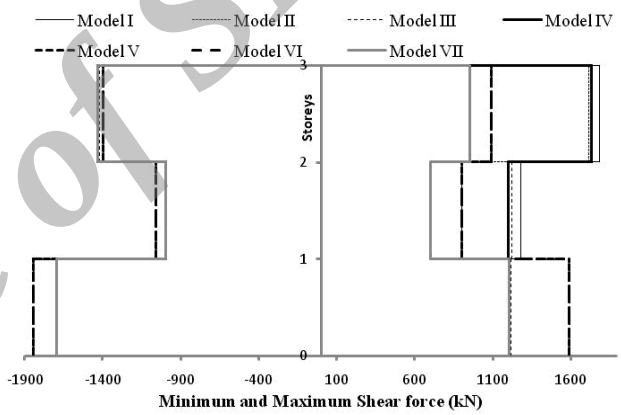


b) Arleta ground excitation

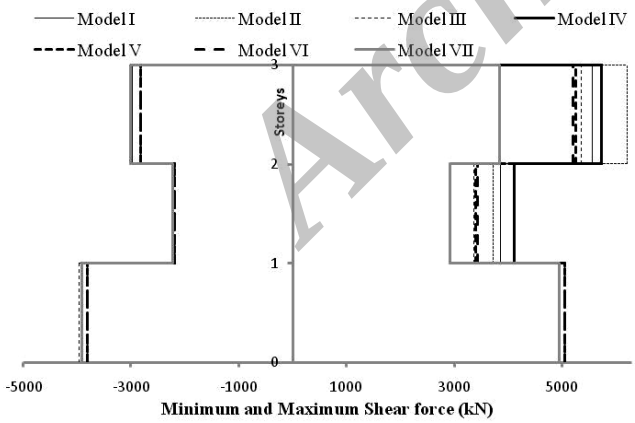


c) Santa Monica excitation

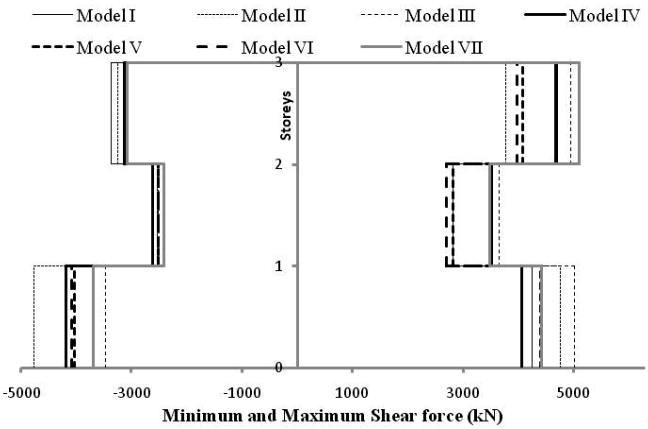


d) Sanfernando excitation

Figure 10. Storey-wise shear forces of right structure

Table 5 shows that at the first storey levels of MDOF stick system pounding forces have not induced in the structures under medium ground excitations like El Centro and Arleta

ground motions, whereas, in high ground motion excitations like Santa Monica and Sanfernando, a lesser magnitude impact force is developed with a very few number of collisions. It is observed that top storey produces more impact forces than the lower ones. The impact forces offered by the left-middle structures are much severe than the middle-right structures that's because of their high in-plane rigidity. Normally, it is seen that by using higher gap element stiffness, the magnitude of impact force increases significantly but number of impacts between the structures become lesser. But here in the study, one peculiar observation is that Model I, II & III suffers high magnitude impact forces than the Model IV, V & VI, although the stiffness used for the gap elements of Model IV, V & VI are quite higher than the Model I, II & III. This could happen because of nonlinear pounding force equations are used to satisfy the condition of dynamic equilibrium. The response of structure is harsher in Santa Monica and Sanfernando earthquakes than any other else due to their significant ground motion characteristics. The Hertz damped model (Model V) and nonlinear viscoelastic model (Model VI), which have nonlinear spring along with the nonlinear dashpot, reduce the pounding forces as compared to the other used nonlinear impact stiffness gap element model i.e. Hertz model (Model IV). Because hertz model cannot dissipate the energy due to the absence of damping constant used in its mathematical formulations of pounding. The models with linear impact spring gap element like linear spring element (Model I), Kelvin-Voigt spring element (Model II) and modified Kelvin-Voigt spring element (Model III) offer almost identical values of impact forces.

From the structural energy plots shown in the Figs. 11, 12 and 13, it is noted that in the end flexible structure the structural energy is mostly dropped down during the presence of pounding than in the absence of pounding. While in the interior and exterior rigid structure, it seems to be augmented in the presence of pounding than in the absence of pounding. In Model II relatively less amount of structural energy is formed than all other considered models. All models of impact simulations have build up almost same amount of structural energy. The variation of structural energy is smaller in rigid structure, while in middle and flexible outer structure it is much higher.

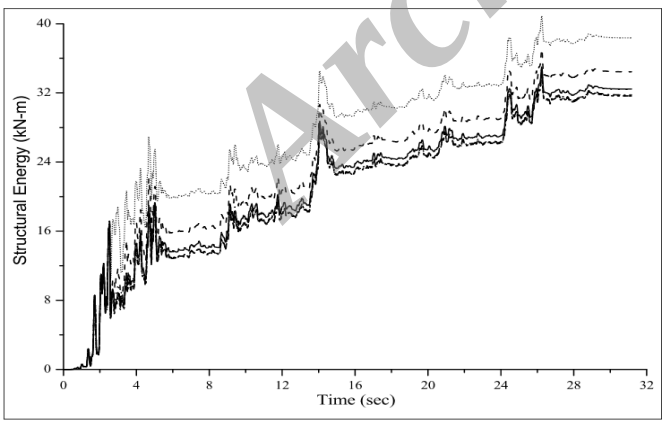


a) El Centro ground excitation

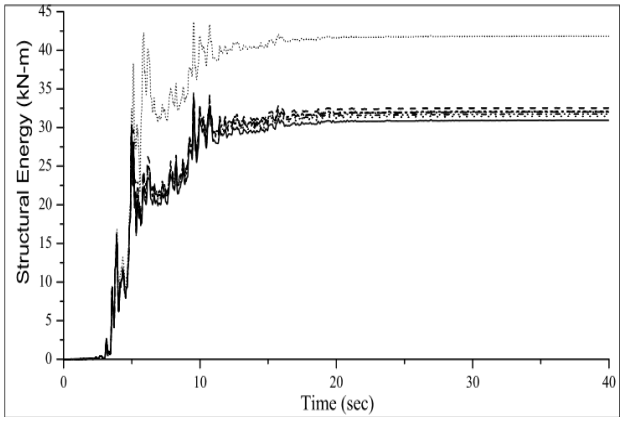


b) Arleta ground excitation

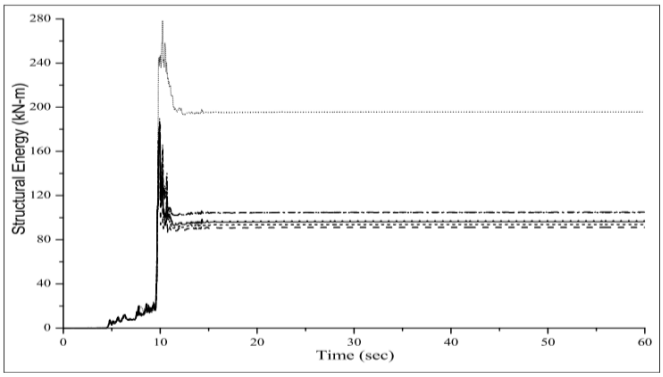


c) Santa Monica excitation

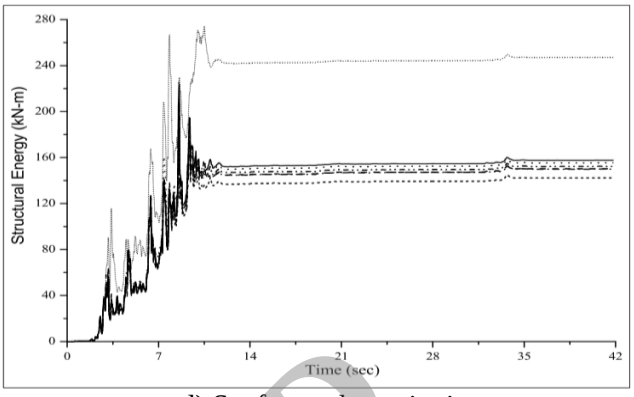


d) Sanfernando excitation

Figure 11. Total structural energy of left structure

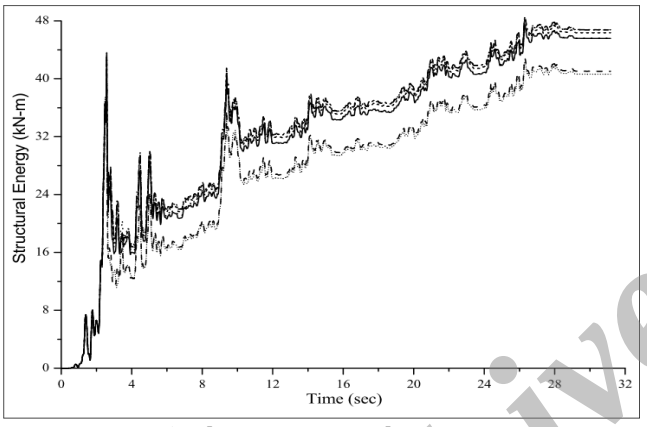


a) El Centro ground excitation

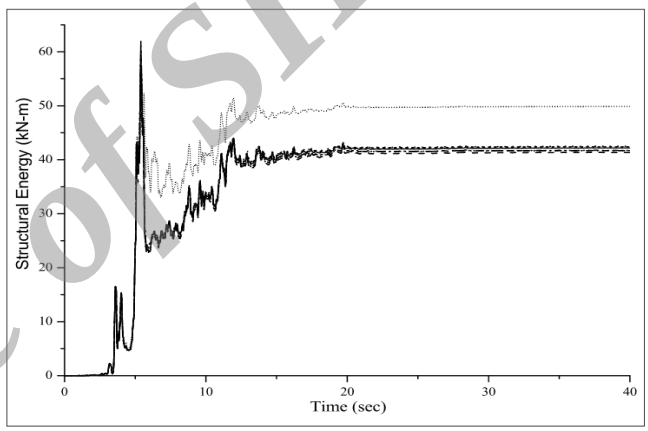


b) Arleta ground excitation

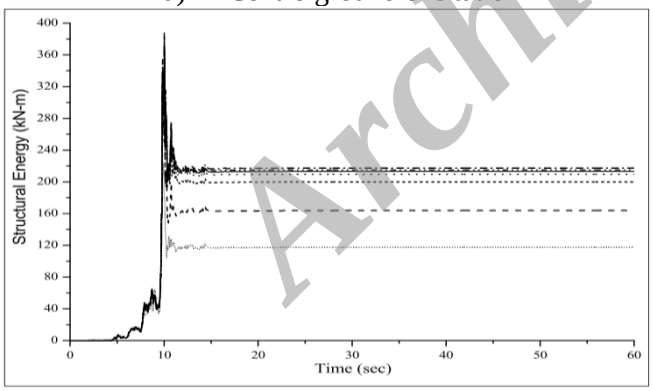


c) Santa Monica excitation

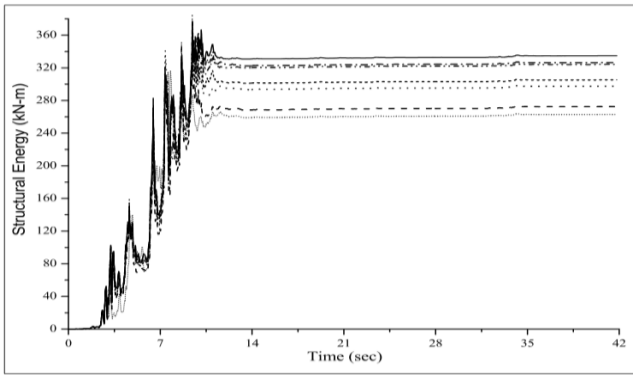


d) Sanfernando excitation

Figure 12. Total structural energy of middle structure

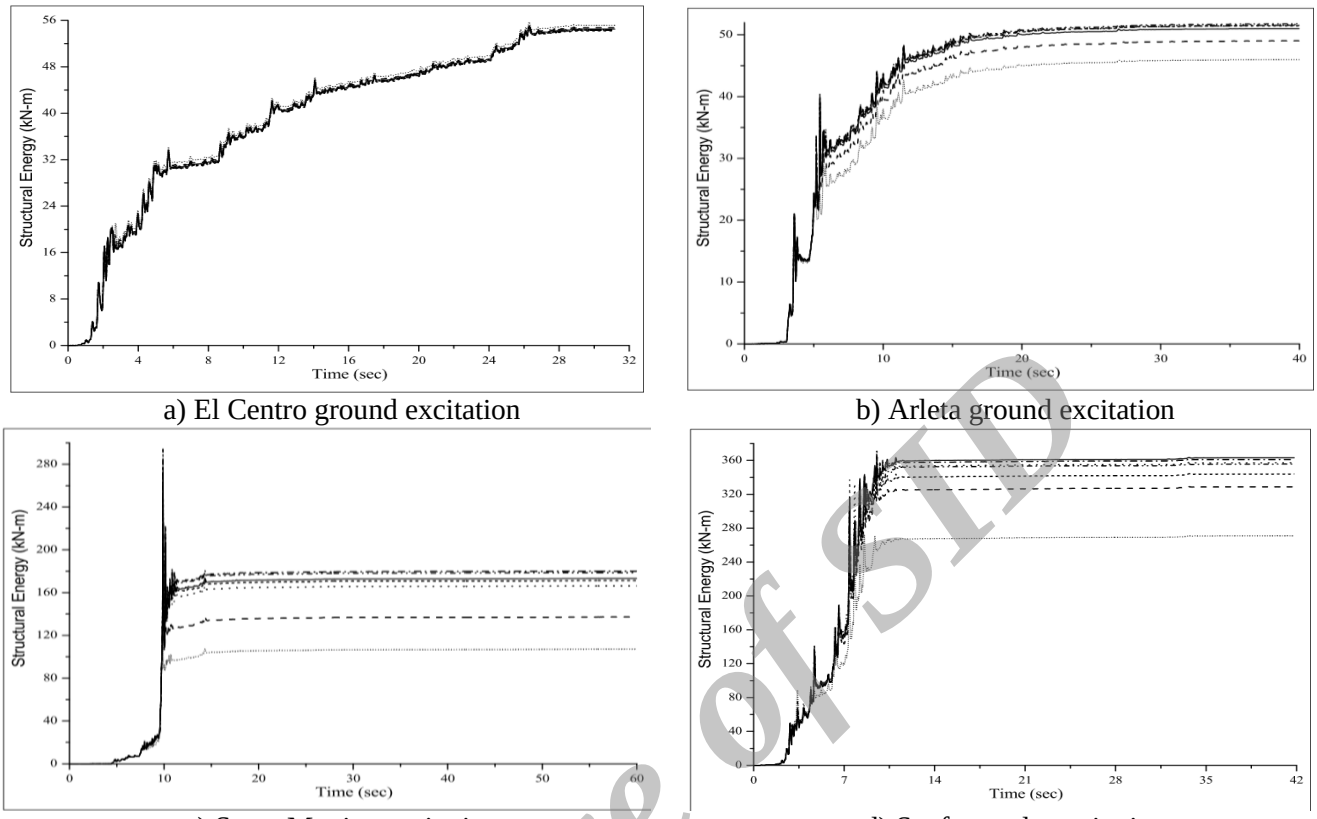


a) El Centro ground excitation b) Arleta ground excitation

c) Santa Monica excitation d) Sanfernando excitation

Figure 13. Total structural energy of right structure

Results presented in Table 6 indicates that in the exterior rigid structure the amount of structural energy transformation is mostly higher in the absence of pounding, while, in the interior and exterior right flexible structures this energy transformation is higher for the case when the pounding is considered. The positive energy (transferred energy) is mostly negligible in all the structures irrespective of absence or presence of pounding. Structural energy is much higher than the input energy under all ground excitations. The energy transformation is almost similar in all the models of impact simulation. Santa Monica and Sanfernando ground excitation impose higher energy interactions in the structures than the other considered ground motions.

Table 6: Maximum energy transformation during pounding for all models under all ground excitations

| Input ground motion | Model No. | Left structure | | Middle structure | | Right structure | |
|---|---|---|---|---|---|---|---|
| | | Positive energy | Negative energy | Positive energy | Negative energy | Positive energy | Negative energy |
| El Centro | I | 0 | 12.5 | 0 | 34.1 | 0 | 20.6 |
| | II | 0 | 14.5 | 0 | 29.4 | 0 | 20.2 |
| | III | 0 | 12.2 | 0 | 32.2 | 0 | 20.2 |
| | IV | 0 | 12.3 | 0 | 33.9 | 0 | 20.4 |

| | | | | | | | |
|---|---|---|---|---|---|---|---|
| | V | 0 | 12.1 | 0 | 34 | 0 | 20.4 |
| | VI | 0 | 12 | 0 | 33 | 0 | 20.3 |
| | VII | 0 | 16.9 | 0 | 26.4 | 0 | 20.7 |
| | I | 0 | 18.7 | 0 | 41.7 | 0 | 27.3 |
| | II | 0 | 18.8 | 0 | 35 | 0 | 23.6 |
| | III | 0 | 18.7 | 0 | 40.7 | 0 | 27.4 |
| Arleta | IV | 0 | 18.5 | 0 | 38.9 | 0 | 27.3 |
| | V | 0 | 18.6 | 0 | 39.2 | 0 | 27.7 |
| | VI | 0 | 18.6 | 0 | 40 | 0 | 28.8 |
| | VII | 0 | 24.2 | 0 | 32.4 | 0 | 20.6 |
| | I | 0 | 99.4 | 0 | 259 | 0 | 180 |
| | II | 7.7 | 109.9 | 0 | 250 | 0 | 177 |
| | III | 0 | 112 | 0 | 254 | 0 | 145.9 |
| Santa Monica | IV | 0 | 92.4 | 0 | 271.5 | 0 | 202.3 |
| | V | 0 | 104 | 0 | 250.9 | 1 | 189.2 |
| | VI | 0 | 104 | 0 | 224.2 | 1 | 186.6 |
| | VII | 0 | 165 | 0 | 144 | 14.6 | 56.2 |
| | I | 8.9 | 105 | 0 | 193 | 0 | 213 |
| | II | 11.1 | 80.7 | 0 | 157 | 0 | 217 |
| | III | 7.5 | 64 | 0 | 202 | 0 | 239 |
| Sanfernando | IV | 1.8 | 95 | 0 | 185 | 0 | 212 |
| | V | 7.6 | 85 | 0 | 191 | 0 | 215 |
| | VI | 13 | 81 | 0 | 167 | 0 | 210 |
| | VII | 0 | 144 | 0 | 172 | 0 | 129 |

(Energy is measured in units of kN-m)

During collision of structures there is sudden break of momentum of the displacement at the pounding levels which results in large and quick short duration acceleration impulses in the opposite direction causing a greater damage to the structures. To study this effect floor spectral acceleration curves for all the three adjoining structures at top storey levels under all ground excitation are plotted in figures 14, 15 and 16. All seven types of impact simulation models with and without pounding have been considered while plotting the floor acceleration spectra.

Through Figs 14, 15 and 16, it is clearly seen that during pounding the spectral acceleration values are much spread for a quite long time period of structure than that of the case of absence of pounding. Right structures have high accelerations than the middle and left structures sequentially, which indicates that the flexible structures suffer more damages than that of rigid structures in pounding. One important observation in all the structures is that after attaining the peak acceleration values of spectra at certain time period range, the further successive values are not getting down considerably, but it remains flatter with high amount of acceleration mostly during pounding. While, in the absence of pounding in these structures there should be only one peak value of acceleration, however, the further successive acceleration values go down instantly with the period of the structures. In flexible structures, it is noted that spectral acceleration values have reduced significantly in the absence of pounding, while in rigid structures these values in the absence of pounding may get amplified in some cases of impact simulation techniques. In exterior flexible right

structures in the presence and absence of pounding, their find minor difference in the peak values of spectral acceleration for all the impact modeling techniques. The results of floor acceleration spectra are found sensitive to the type of impact simulation techniques adopted for pounding response of structures.

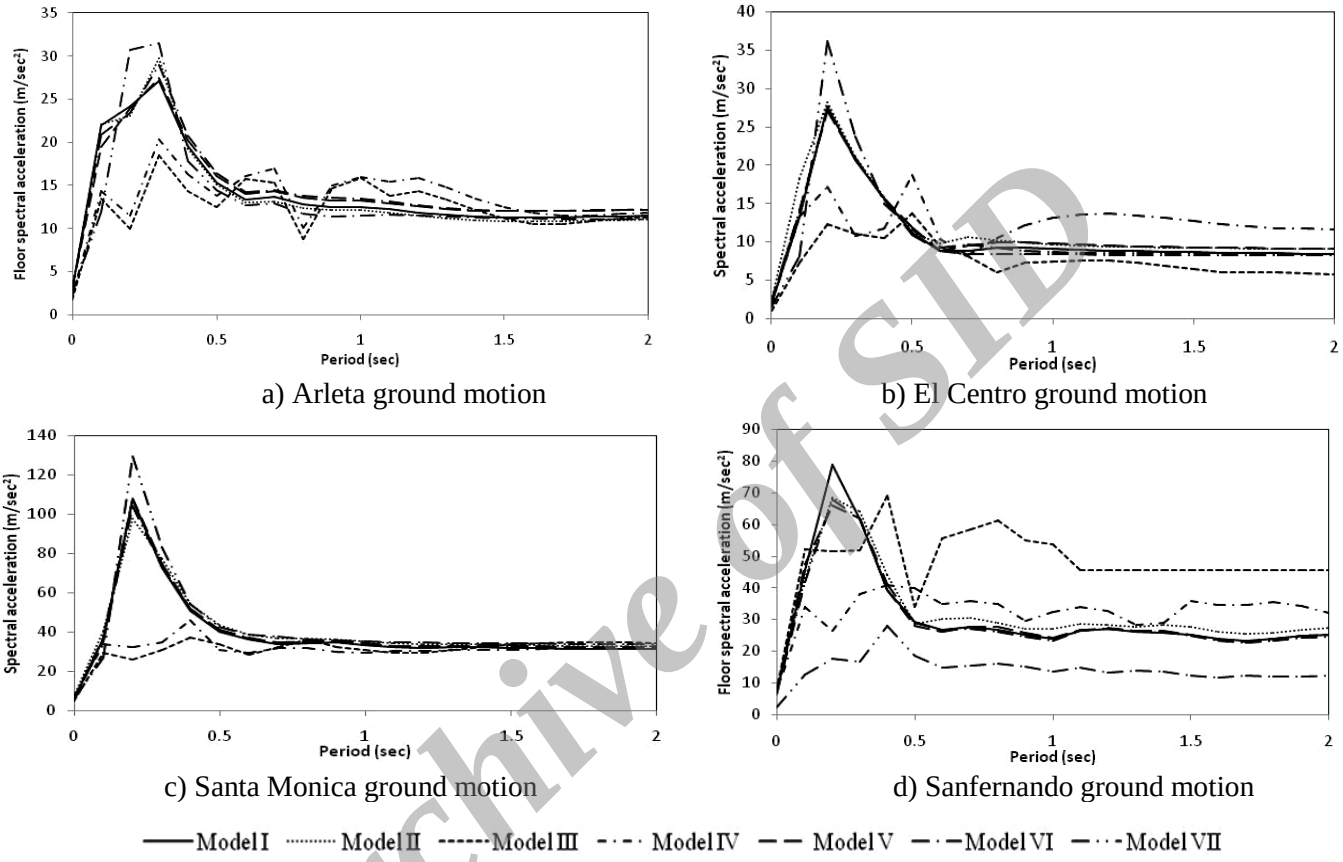


a) Arleta ground motion

b) El Centro ground motion

c) Santa Monica ground motion

d) Sanfernando ground motion

Figure 14. Floor acceleration time spectra of left structure for gap of 0.01 m at top storey level

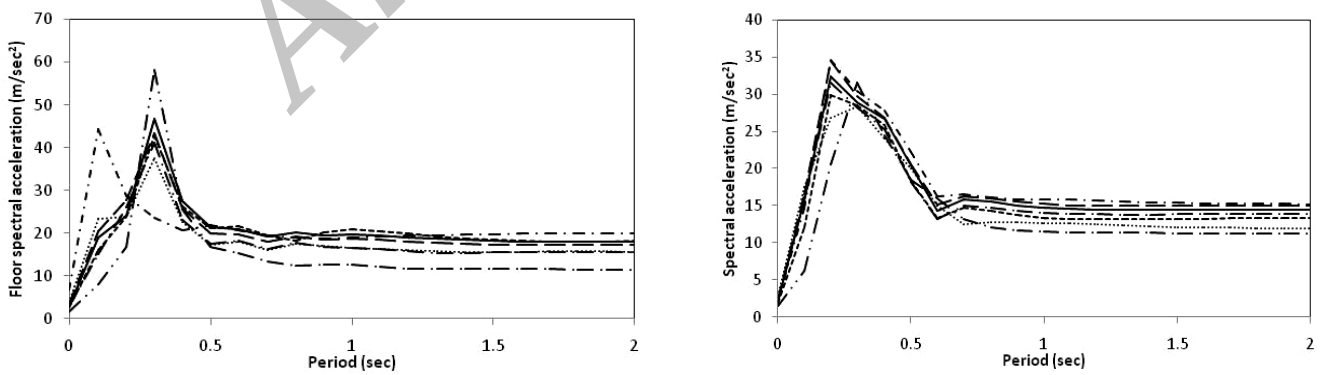


a) Arleta ground motion

b) El Centro ground motion

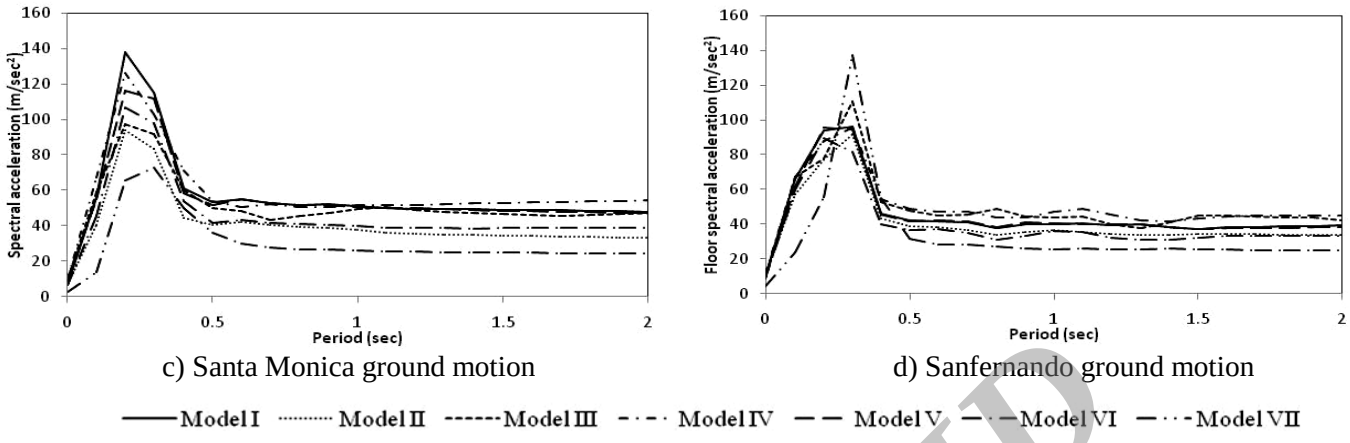


c) Santa Monica ground motion

d) Sanfernando ground motion

Figure 15. Floor acceleration time spectra of middle structure for gap of 0.01 m at top storey level

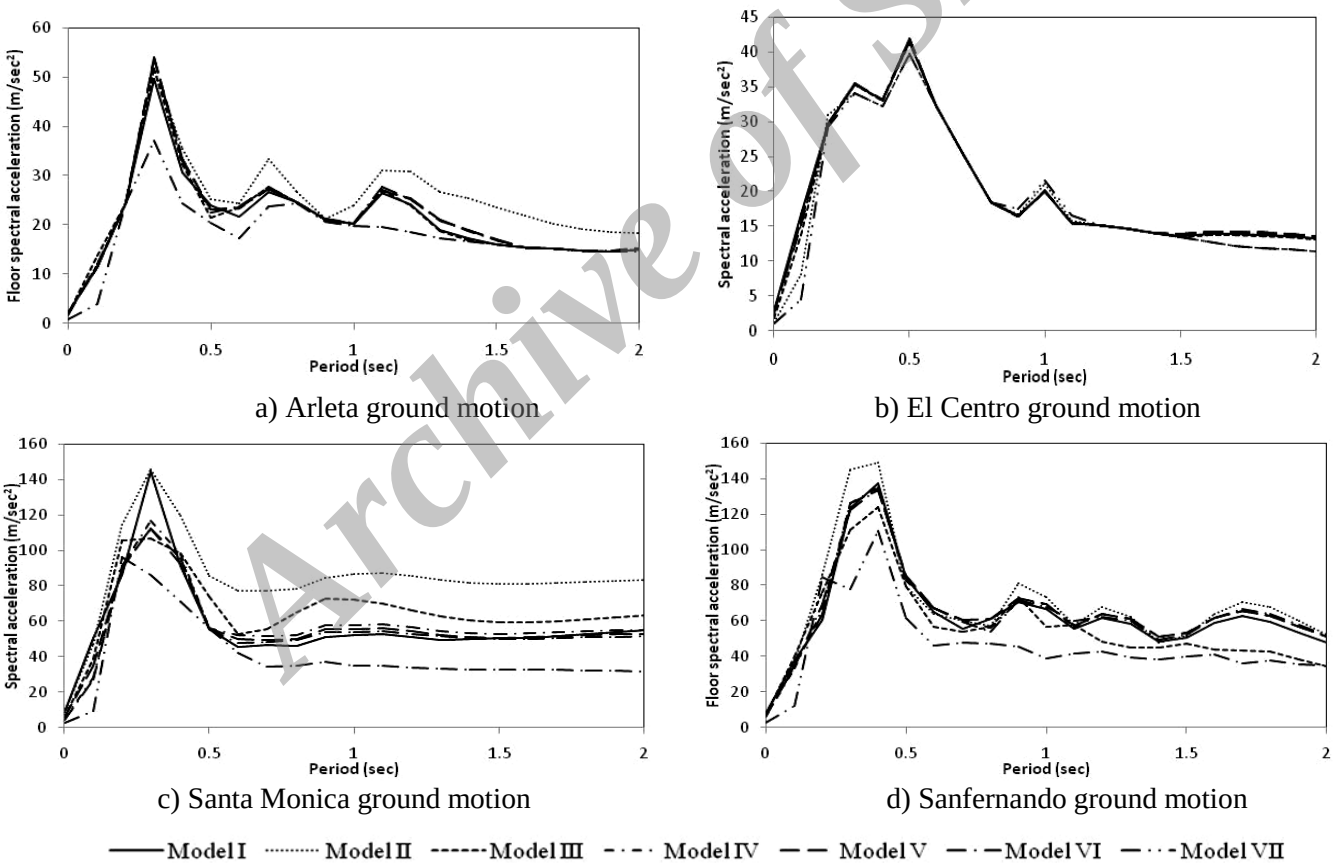


a) Arleta ground motion

b) El Centro ground motion

c) Santa Monica ground motion

d) Sanfernando ground motion

Figure 16. Floor acceleration time spectra of right structure for gap of 0.01 m at top storey level

Furthermore, the time history plots of displacement and impact force for the interaction of top storey levels between left, middle and right structure under San Fernando earthquake

ground excitation for all the models are shown in Figs. 17 to 21. The same figures can also reflects the validation of SAP results with respect to MATLAB results of Model I. Already these plot results are conferred and taken in care in the entire above section.

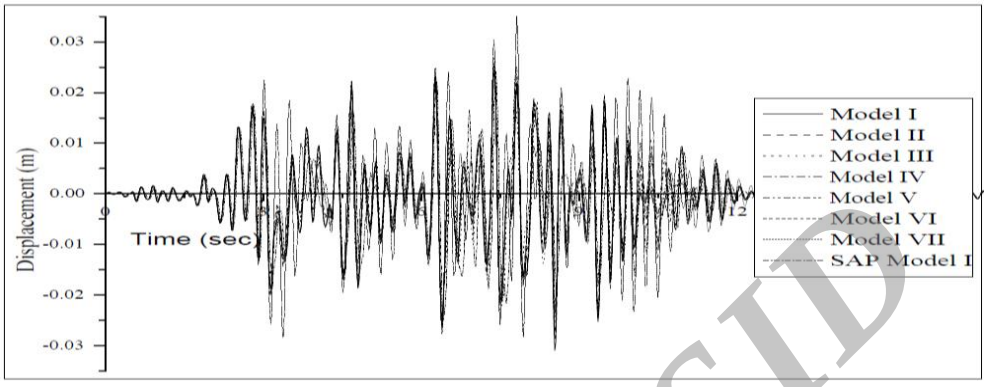


Figure 17. Top storey displacement time history plot of left structure under Sanfernando ground excitation

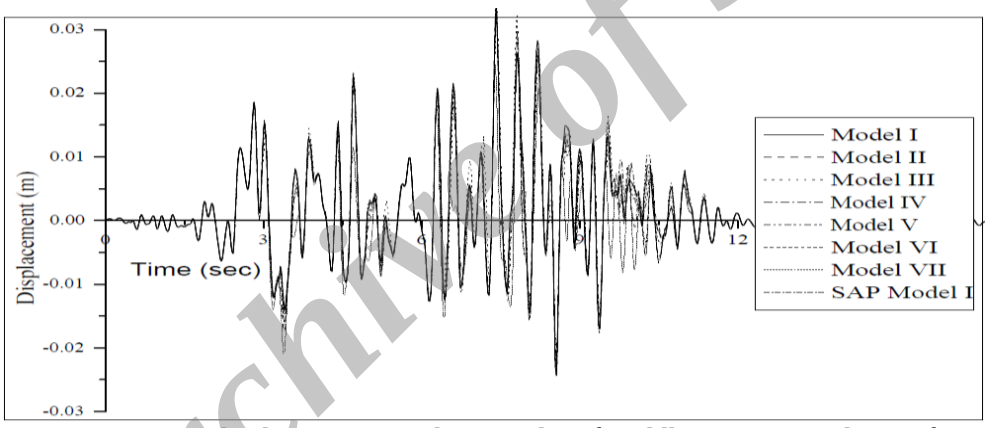


Figure 18. Top storey displacement time history plot of middle structure under Sanfernando ground excitation

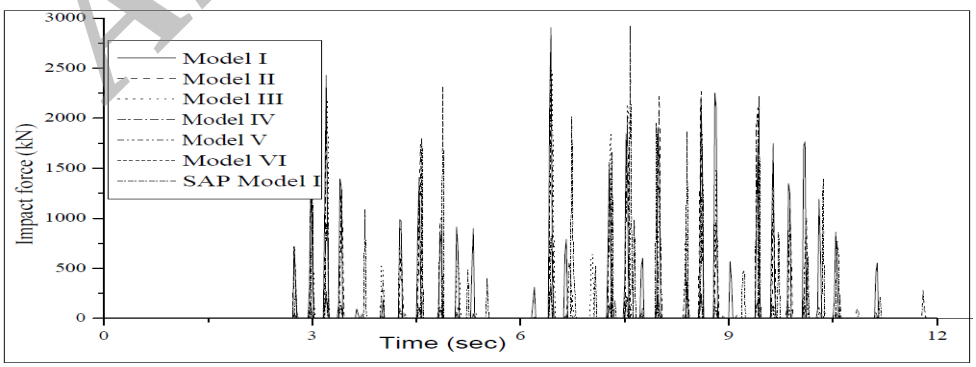


Figure 19. Top storey displacement time history plot of right structure under Sanfernando ground excitation

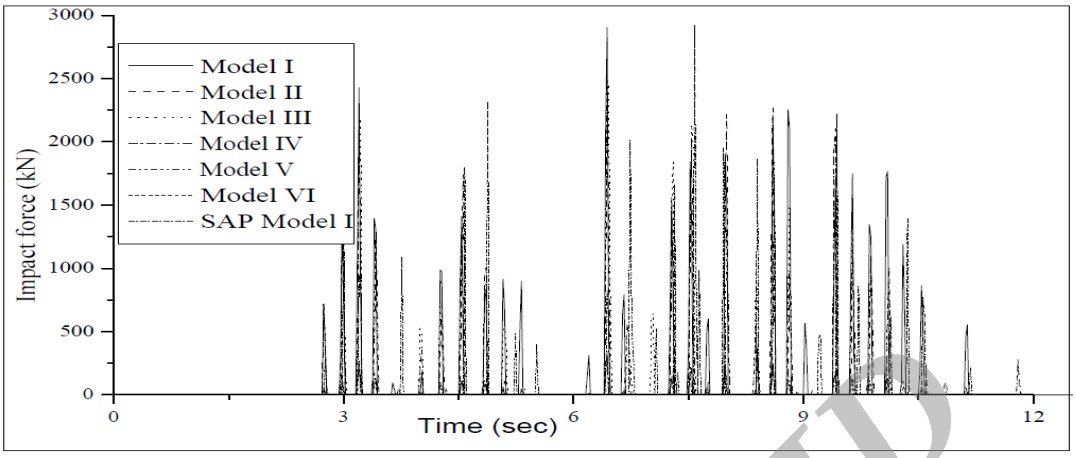


Figure 20. Top storey pounding force time history plot for the interaction between middle-right structure under Sanfernando ground excitation

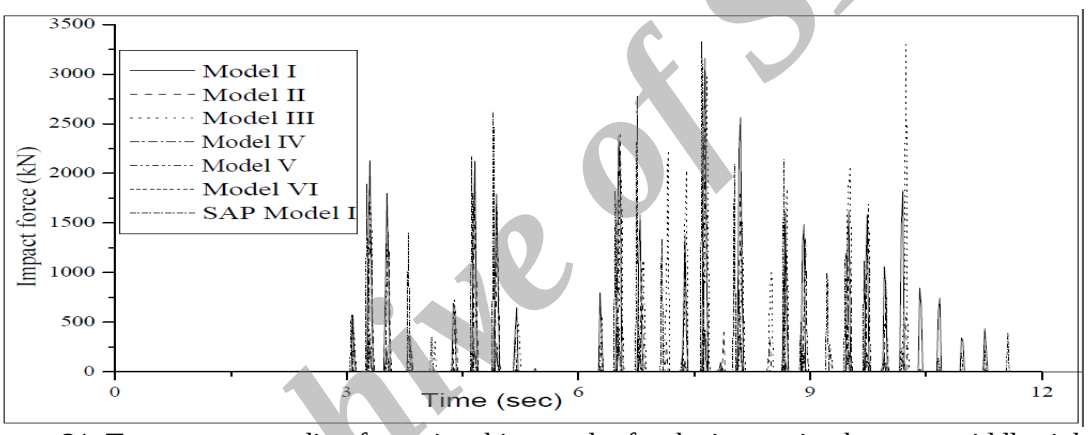


Figure 21. Top storey pounding force time history plot for the interaction between middle-right structure under Sanfernando ground excitation

## 7. CONCLUSIONS

The behavior of three adjacent MDOF structures with various linear and non linear spring stiffness contact elements for impact simulation is investigated under four real earthquake ground excitations assuming a linear elastic behavior of the structures. The governing equation of motion of MDOF stick models are formulated and solved using a program prepared in MATLAB, which is also verified using FE analysis package, SAP 2000 NL. For impact simulation of MDOF structures, six different contact elements namely linear spring element, Kelvin-Voigt element, Modified Kelvin-Voigt element, Hertz contact element, Hertz damp contact element and nonlinear viscoelastic contact element are used and studied. MDOF stick model response is also evaluated for varying parameter like time step size of time history analysis considering El Centro ground motion and linear spring contact element only to simulate the seismic pounding response. Based on the trends of the result obtained from the numerical study following precise conclusions can be made:

i. Displacement response of structure in all models of impact simulations are more or less same, so using different kinds of impact simulation technique there is minimal change in the peak displacement response of a structure.

ii. Row building in series, subjected to pounding action, it was found that the exterior right flexible structure of the series in the direction of applied ground excitation offers very untraditional pattern of absolute shear forces. That means top storey of this structure may have more values of shear forces than the immediate lower storey, which is very uncommon in regular structures.

iii. All contact elements of linear spring stiffness exhibit the same type of impact forces in the structure, in magnitude wise and in numbers. Whereas for the gap element of nonlinear spring stiffness, it is found that the Hertz damped and nonlinear viscoelastic impact simulation techniques offer less pounding forces.

iv. Nonlinear spring stiffness used for impact simulation of adjacent structures like Hertz, Hertz damped and nonlinear viscoelastic techniques offer less magnitude impact forces in the structure at collision levels than the linear spring stiffness used for the impact simulation of adjacent structures. On the other hand the values of peak displacement of all the models of impact simulation at the time of collisions were found to be marginally same.

v. The presence of impact forces in the closely space structures have drastically increased the spectral acceleration of the structural system. Also the peak spectral acceleration values in case of pounding are significantly spread up for a quite long structural period range than that in the absence of pounding.



## REFERENCES

1. Rosenblueth E, Meli R. The 1985 earthquake: causes and effects in Mexico City, *Concrete International*, No. 5, **8**(1986) 23-4.
2. Kasai K, Jeng V, Patel PC, Munshi JA, Maison BF. Seismic pounding effects- survey and analysis, *Proceeding of 10th World Conference on Earthquake Engineering*, Madrid, Spain, 1992, pp. 3893-3898.
3. Gokhale VA, Joshi D. Vulnerability assessment of building stock at historic city of Pune, India. With reference to pounding hazard, *Proceeding of 15th World Conference on Earthquake Engineering*, Lisbon, Portugal, 2012, Paper No. 2072.
4. Anagnostopoulos SA. Pounding of buildings in series during earthquakes, *Earthquake Engineering and Structural Dynamics*, **16**(1988) 443-56.
5. Pantelides P, Ma X. Linear and nonlinear pounding of structural systems, *Computers & Structures*, No. 1, **66**(1998) 79-92.
6. Wang LX, Chau KT. Chaotic seismic torsional pounding between two single storey asymmetric towers, *Proceeding of 14th World Conference on Earthquake Engineering*, Beijing, China, October 12-17, 2008.

7. Davis RO. Pounding of buildings modeled by an impact oscillator, *Earthquake Engineering and Structural Dynamics*, **21**(1992) 253-74.
8. Xing S, Halling MW, Meng Q. Structural pounding detection by using wavelet scalogram, *Advances in Acoustics and Vibration*, Article ID 805141, Doi:10.1155/2012/805141, 2012, 10 p.
9. Maison BF, Kasai K. Dynamics of pounding when two buildings collide, *Earthquake Engineering and Structural Dynamics*, **21**(1992) 771-86.
10. Kun Y, Li L, Hongping Z. A modified Kelvin impact model for pounding simulation of base isolated building with adjacent structures, *Earthquake Engineering and Engineering Vibration*, No. 3, **8**(2009) 433-46.
11. Moustafa A, Mahmoud S. Damage assessment of adjacent buildings under earthquake loads, *Engineering Structures*, No. 1, **61**(2014) 153-65.
12. Papadrakakis M, Mouzakis P. Three dimensional nonlinear building pounding with friction during earthquakes, *Journal of Earthquake Engineering, Imperial College Press*, No. 1, **8**(2004) 107-32.
13. Pant R, Wijeyewickrema AC. Seismic pounding between reinforced concrete buildings: A study using recently proposed contact element models, *Proceeding of the 14th European Conference on Earthquake Engineering*, Republic of Macedonia, 2010.
14. Rojas FR, Anderson JC. Pounding of an 18 storey building during recorded earthquakes, *ASCE Journal of Structural Engineering*, No. 12, **138**(2012) 1530-44.
15. Jameel M, Saiful Islam ABM, Hussain RR, Hasan SD, Khaleel M. Nonlinear FEM analysis of seismic induced pounding between neighboring multi-storey structures, *Latin American Journal of Solids and Structures*, **10**(2013) 921-39.
16. Matsagar VA, Jangid RS. Seismic response of base-isolated structures during impact with adjacent structure, *Engineering Structures*, **25**(2003) 1311-23.
17. Agarwal VK, Niedzwecki JM, Vandelindt JW. Earthquake induced pounding in friction varying base isolated buildings, *Engineering Structures*, **29**(2007) 2825-32.
18. Komodromos P, Polycarpou PC, Papaloizou L, Phocas MC. Response of seismically isolated buildings considering poundings, *Earthquake Engineering and Structural Dynamics*, **36**(2007) 1605-22.
19. Chau KT, Wei XX, Guo X, Shen CY. Experimental and theoretical simulations of seismic poundings between two adjacent structures, *Earthquake Engineering and Structural Dynamics*, **32**(2003) 537-54.
20. Valles-Mottex RE, Reinhorn AM. An energy approach to pounding of structures, *Proceeding of 11th World Conference on Earthquake Engineering*, Acapulco, Mexico, 1996, Paper No. 2106.
21. MATLAB - The Language of Technical Computing, Getting started with MATLAB, Version R2009b, The Mathworks, 2009.
22. SAP User's Manual (Structural Analysis Program), Computers and Structures Inc. University Ave, Berkeley CA, 1995.
23. Athanassiadou CJ, Penelis GG, Kappos AJ. Seismic response of adjacent buildings with similar or different dynamic characteristics, *Earthquake Spectra*, No. 2, **10**(1994) 293-317.
24. Papadrakakis M, Mouzakis H, Plevris N, Bitzarakis S. A Lagrange multiplier solution method for pounding of buildings during earthquakes, *Earthquake Engineering and Structural dynamics*, **20**(1991) 981-98.

25. Muthukumar S, DesRoches RA. Hertz contact model with nonlinear damping for pounding simulation, *Earthquake Engineering and Structural Dynamics,* **35**(2006) 811-28.
26. Jankowski R. Pounding force response spectrum under earthquake excitation, *Engineering Structures,* **28**(2006) 1149-61.
27. Mahmoud S, Jankowski R. Modified linear viscoelastic model of earthquake induced structural pounding, *IJST-Transaction of Civil and Environmental Engineering*, No. C1, **35**(2011) 51-62.
28. Barros RC, Khatami SM. An estimation of damping ratio for the numerical study of impact forces between two adjacent concrete buildings subjected to pounding, *Proceedings of 15th International Conference on Experimental Mechanics*, Porto, Portugal, Paper Ref. 4051, 22-27th July, 2012.